Moduli spaces for Lamé functions and Abelian differentials of the second kind

Alexandre Eremenko[*], Andrei Gabrielov[*],
Gabriele Mondello[†] and Dmitri Panov[‡]

June 30, 2020

Abstract

Topology of the moduli space for Lamé functions of degree m is determined: this is a Riemann surface which consists of two connected components when $m \geq 2$; we find the Euler characteristics and genera of these components. As a corollary we prove a conjecture of R. Maier on degrees of Cohn's polynomials. These results are obtained with the help of a geometric description of these Riemann surfaces, as quotients of the moduli spaces for certain singular flat triangles.

An application is given to the study of metrics of constant positive curvature with one conic singularity with the angle $2\pi(2m+1)$ on a torus. We show that the degeneration locus of such metrics is contained in the union of smooth analytic curves and enumerate these curves.

2010 MSC: 33E10, 30F30, 57M50.

Keywords: Plane algebraic curve, elliptic curve, Lamé equation, Abelian differential, translation surface, flat metric, spherical metric, conic singularity.

[*]Supported by NSF grant DMS-1665115.

[†]Partially supported by INdAM and by grant PRIN 2017 "Moduli and Lie theory".

[‡]Supported by EPSRC grant EP/S035788/1.

1 Introduction

1.1 Statement of main results

Consider an elliptic curve in the form of Weierstrass

$$u^2 = 4x^3 - g_2 x - g_3, \quad g_2^3 - 27g_3^2 \neq 0. \tag{1}$$

Lamé equation (algebraic version) is the second order differential equation

$$\left(\left(u\frac{d}{dx} \right)^2 - m(m+1)x - \lambda \right) w = 0, \tag{2}$$

where $m \geq 0$ is an integer. The more familiar form of the Lamé equation is

$$\frac{d^2W}{dz^2} - \left(m(m+1)\wp(z) + \lambda \right) W = 0, \tag{3}$$

which is obtained from (2) by the change of the independent variable $x = \wp(z),\ u = \wp'(z),\ W(z) = w(\wp(z))$. Here $\wp$ is the Weierstrass function of the lattice Λ with invariants

$$g_2 = 60 \sum_{\omega \in \Lambda \setminus \{0\}} \omega^{-4}, \quad g_3 = 140 \sum_{\omega \in \Lambda \setminus \{0\}} \omega^{-6}.$$

Changing the variables in (2) to $x_1 = kx,\ w_1(x_1) = w(x_1/k)$, we obtain a new equation (2) with parameters

$$(k\lambda, k^2 g_2, k^3 g_3), \quad k \in \mathbf{C}^*. \tag{4}$$

Two equations obtained by such a change of the variables are called *equivalent.* The set of equivalence classes is the *moduli space for Lamé equations*, Lame_m. The quotient of $\mathbf{C}^3 \setminus \{0\}$ by the $\mathbf{C}^*$ action (4) is the weighted projective space $\mathbf{CP}(1,2,3)$, see for example [16], and Lame_m is obtained from it by removing the curve $g_2^3 - 27g_3^2 = 0$. It parametrizes projective structures on tori with one conic singularity with conic angle $2\pi(2m+1)$. For a general discussion of projective structures with conic singularities we refer to [24]. Lame_m has two singularities corresponding to two points with non-trivial stabilizers: $(0,1,0)$ and $(0,0,1)$, which correspond to square and hexagonal tori in (1).

The homogeneous function

$$J = \frac{g_2^3}{g_2^3 - 27g_3^2}$$

is called the *absolute invariant* of the elliptic curve (1); it defines a map $\pi_m : \mathrm{Lame}_m \to \mathbf{C}_J$ which is called the *forgetful map*.

A *Lamé function* is a non-trivial solution w of (2) with the property that w^2 is a polynomial. It is easy to see that the degree of this polynomial must be m. Such solutions exist if and only if the *accessory parameter* λ satisfies an algebraic equation

$$F_m(\lambda, g_2, g_3) = 0, \tag{5}$$

where F_m is a polynomial in three variables, monic with respect to λ, which is invariant under the $\mathbf{C}^*$ action (4). For each λ satisfying (5), the Lamé function is unique up to a constant factor, [30, 23.41].

Two Lamé functions are *equivalent* if $w(x) = cw_1(kx),\ c, k \in \mathbf{C}^*$, and the set of equivalence classes is the *moduli space for Lamé functions* $\mathbf{L}_m \subset \mathrm{Lame}_m$. We consider this space $\mathbf{L}_m$ as an abstract Riemann surface which is obtained by taking the quotient of the surface

$$\{(\lambda, g_2, g_3) \in \mathbf{C}^3 : F_m(\lambda, g_2, g_3) = 0,\ g_2^3 - 27g_3^2 \neq 0\}$$

by the $\mathbf{C}^*$ action (4). It is the normalization of the curve defined by equation (5) in $\mathbf{CP}(1,2,3)\backslash\{g_2^3 - 27g_3^2 = 0\}$. Since F_m in (5) is a monic polynomial, the forgetful map $\mathbf{L}_m \to \mathbf{C}_J$ is proper.

Equations (5) for $m \leq 8$ are explicitly written in Table 3 in [23], see also Appendix to the present paper. Maier calls F_m the *Lamé spectral polynomials*.

Lamé equation and Lamé functions have long history going back to the work of Gabriel Lamé [19, 20], and they have been intensively studied ever since, because of their importance for mathematical physics. Good reference for the classical work is [30], and a modern survey is contained in the first three sections of [23].

Most of the classical work on Lamé functions was concentrated on the real case with positive discriminant (g_2, g_3, λ are real and $g_2^3 - 27g_3^2 > 0$), and we are not aware of any systematic study of general properties of F_m and $\mathbf{L}_m$.

In this paper we determine the topology of the Riemann surfaces $\mathbf{L}_m$. To state our main result, we recall the notion of a 2-dimensional orbifold [7],[27].

It is a compact Riemann surface S with a function $n : S \to \mathbf{N}_{\geq 1} \cup \{\infty\}$, where $\mathbf{N}_{\geq 1}$ is the set of positive integers, such that $n(z) = 1$ for all points, except finitely many *orbifold points* of order $n(z) > 1$. Points with $n(z) = \infty$ are the punctures. For example, the moduli space for tori $\mathbf{C}_J$ has a natural orbifold structure with $S = \overline{\mathbf{C}}$ and three orbifold points: $n(0) = 3$, $n(1) = 2$, and $n(\infty) = \infty$. $J = 0$ corresponds to the hexagonal torus, and $J = 1$ to the square torus.

The orbifold Euler characteristic is defined as

$$\chi^O = \chi(S) - \sum (1 - 1/n(z)) \,,$$

where $\chi(S) = 2 - 2g(S)$ is the ordinary Euler characteristic of the underlying compact surface, and g is the genus. A ramified covering $f : S_1 \to S_2$ is called an *orbifold map* if $n(f(x))$ divides $n(x) \deg_z(f)$ for all $x \in S_1$, and an *orbifold covering* if

$$n(f(x)) = n(x) \mathrm{ord}_x f \quad \text{for all} \quad x \in S_1. \tag{6}$$

If f is an orbifold covering, the Riemann-Hurwitz formula gives

$$\chi^O(S_1) = \deg(f) \chi^O(S_2). \tag{7}$$

We introduce the following functions on non-negative integers m.

$$d_m^I := \begin{cases} m/2 + 1, & m \equiv 0 \pmod 2 \\ (m-1)/2, & m \equiv 1 \pmod 2, \end{cases} \tag{8}$$

$$d_m^{II} := 3\lceil m/2 \rceil. \tag{9}$$

It is easy to see that d_m^I and d_m^{II} always have opposite parity: when $m \in \{0, 3\} \pmod 4$, d_m^I is odd and d_m^{II} is even; when $m \in \{1, 2\} \pmod 4$, d_m^I is even and d_m^{II} is odd.

$$\epsilon_0 = \begin{cases} 0, & \text{if } m \equiv 1 \pmod 3, \\ 1 & \text{otherwise,} \end{cases} \tag{10}$$

$$\epsilon_1 = \begin{cases} 0, & \text{if } m \in \{1, 2\} \pmod 4, \\ 1 & \text{otherwise.} \end{cases} \tag{11}$$

One can restate the definitions of ϵ_j as follows: $\epsilon_0 = 0$ if and only if d_m^I is divisible by 3, and $\epsilon_1 = 0$ if and only if d_m^I is even.

Our main result is the following.

Theorem 1.1. *When $m \geq 2$, $\mathbf{L}_m$ is a Riemann surface consisting of two connected components which we call $\mathbf{L}_m^I$ and $\mathbf{L}_m^{II}$, while $\mathbf{L}_0$ and $\mathbf{L}_1$ are connected: $\mathbf{L}_0 = \mathbf{L}_0^I$ and $\mathbf{L}_1 = \mathbf{L}_1^{II}$.*

Riemann surface $\mathbf{L}_m$ has a natural orbifold structure with ϵ_0 orbifold points of order 3 on $\mathbf{L}_m^I$, and one orbifold point of order 2 which belongs to $\mathbf{L}_m^I$ when $\epsilon_1 = 1$ and to $\mathbf{L}_m^{II}$ otherwise. Component $\mathbf{L}_m^I$ has d_m^I punctures, and component $\mathbf{L}_m^{II}$ has $2d_m^{II}/3 = 2\lceil m/2 \rceil$ punctures.

Restrictions of the forgetful map to these components are orbifold maps and their degrees are d_m^I and d_m^{II}. The orbifold Euler characteristics are

$$\chi^O(\mathbf{L}_m^I) = -(d_m^I)^2/6 \quad \textit{and} \quad \chi^O(\mathbf{L}_m^{II}) = -(d_m^{II})^2/18. \tag{12}$$

Remark. Ordinary Euler characteristics χ are obtained from the χ^O by adding the *orbifold corrections* which in our case are

$$E^I = (4\epsilon_0 + 3\epsilon_1)/6 \quad \text{and} \quad E^{II} = (1 - \epsilon_1)/2. \tag{13}$$

Euler characteristics can be expressed as functions of m rather than d, see Appendix.

It is well known that for $m \geq 2$ each polynomial F_m factors into four factors in $\mathbf{C}[\lambda, e_1, e_2, e_3]$, where e_i are related to g_2, g_3 by the equation

$$4x^4 - g_2 x - g_3 = 4(x - e_1)(x - e_2)(x - e_3),$$

see for example [29, Thm. 2] for an explicit statement of this. However there is no discussion of irreducibility of these four factors in the literature. Our theorem says that for $m \geq 2$, F_m has exactly two irreducible factors in $\mathbf{C}[\lambda, g_2, g_3]$ and implies that the four factors of F_m in $\mathbf{C}[\lambda, e_1, e_2, e_3]$ are irreducible.

Theorem 1.1 implies the formulas for the genera of $\mathbf{L}_m^K$, $K \in \{I, II\}$ in terms of m or d_m^K which are given in the Appendix.

We give several applications of Theorem 1.1. As a first application, we prove that the two irreducible components of the surface $F_m(\lambda, g_2, g_3) = 0$ in (5) have no singularities in $\mathbf{C}^3$ except the lines $(0, t, 0)$ and $(0, 0, t)$.

To obtain a non-singular curve in $\mathbf{CP}^2$ parametrizing $\mathbf{L}_m$, we use Legendre's family of elliptic curves

$$v^2 = z(z-1)(z-a), \quad a \in \mathbf{C}_a := \mathbf{C}\backslash\{0, 1\}. \tag{14}$$

For the J-invariant of this curve we have

$$J = \psi(a) = \frac{4}{27}\frac{(a^2-a+1)^3}{a^2(1-a)^2}. \tag{15}$$

If $\overline{\mathbf{C}}_J$ is considered as an orbifold with $n(0) = 3$, $n(1) = 2$, $n(\infty) = \infty$, and in $\overline{\mathbf{C}}_a$ we set $n(a) = \infty$ for $a \in \{0, 1, \infty\}$, and $n(a) = 1$ otherwise, then $\psi \mapsto J(a)$ is an orbifold covering.

The form of the Lamé equation corresponding to (14) is

$$Py'' + \frac{1}{2}P'y' - ((m(m+1)z + B)y = 0, \quad P(z) = 4z(z-1)(z-a), \tag{16}$$

where the accessory parameter B is an affine function of λ (see Section 8 for the details of this transformation). Lamé functions correspond to non-trivial solutions y of (16) such that y^2 is a polynomial in z of degree m. For such a solution to exist, a polynomial equation

$$H_m(B, a) = 0 \tag{17}$$

must be satisfied. The Riemann surface defined by this equation will be denoted by $\mathbf{H}_m$. For $m \geq 2$, we will show that it consists of four irreducible components, $\mathbf{H}_m^j$, $j \in \{0, 1, 2, 3\}$. These components are defined as follows: $\mathbf{H}_m^0$ corresponds to polynomial solutions y when m is even and to solutions of the form $y = Q\sqrt{P}$ when m is odd. The other three components $j \in \{1, 2, 3\}$ correspond to solutions

$$Q(z)\sqrt{z}, \quad Q(z)\sqrt{z-1}, \quad Q(z)\sqrt{z-a}, \quad \text{when} \quad m \quad \text{is odd},$$

and

$$Q(z)\sqrt{(z-1)(z-a)}, \quad Q(z)\sqrt{z(z-a)}, \quad Q(z)\sqrt{z(z-1)},$$

when m is even, where Q is a polynomial. The forgetful maps $\sigma_m^j : \mathbf{H}_m^j \to \mathbf{C}_a$ are defined by $(B, a) \mapsto a$.

Polynomial H_m is a product of four factors H_m^j, and we have ramified coverings $\Psi_m^0 : \mathbf{H}_m^0 \to \mathbf{L}_m^I$, and $\Psi_m^j : \mathbf{H}_m^j \to \mathbf{L}_m^{II}$, $j \in \{1, 2, 3\}$ such that

$$\pi_m^K \circ \Psi_m^j = \psi \circ \sigma_m^j,$$

where $\pi_m^K : \mathbf{L}_m^K \to \mathbf{C}_J$ and $\sigma_m^j : \mathbf{H}_m^j \to \mathbf{C}_a$ are the forgetful maps, and ψ is the function (15). We will show that these maps Ψ_m^j, are orbifold coverings

with respect to the appropriate orbifold structures defined on appropriate compactifications of $\mathbf{L}_m^K$ and $\mathbf{H}_m^j$.

This will permit us to compute the genera of components of $\mathbf{H}_m$ via the Riemann–Hurwitz formula. Once the genera and degrees are known one can conclude that these curves are non-singular by the "genus–degree formula":

$$g \leq (d-1)(d-2)/2, \tag{18}$$

where we have equality only for non-singular curves. We consider compactifications $\overline{\mathbf{H}}_m^j$: these are curves in $\mathbf{CP}^2$ defined by homogenizations of equations (17).

Theorem 1.2. *The curves $\overline{\mathbf{H}}_m^j$, $j \in \{0, \ldots, 3\}$ in $\mathbf{CP}^2$ are non-singular, in particular they are irreducible. The degrees of the ramified coverings Ψ_m^j are 6 for $j = 0$ and 2 for $j \in \{1, 2, 3\}$.*

So we have interesting sequences of non-singular planar curves $\overline{\mathbf{H}}_m^j$ defined over $\mathbf{Q}$ for which degrees and genera have been explicitly determined. Only a few such examples of high genus are known to the authors, see [8], [6].

One can deduce Theorem 1.1 from Theorem 1.2: if we know that $\overline{\mathbf{H}}_m^j$ are non-singular, we can find their genera from the equality in (18) and obtain all topological characteristics of $\mathbf{L}_m$ using the orbifold coverings Ψ_m^j.

Corollary 1.1. *Irreducible components of the surfaces (5) have no other singularities except the lines $(0, t, 0)$ and $(0, 0, t)$.*

These results allow us to prove a conjecture of Maier about degrees of Cohn's polynomials [23, Conj. 3.1(ii)]. We recall the definition. Let $F_m = F_m^I F_m^{II}$ be the irreducible factorization. Let D_m^K be the discriminant of F_m^K with respect to λ. Then $D_m^K(g_2, g_3)$ is quasi-homogeneous, that is the curves $D_m^K(g_2, g_3) = 0$ are invariant under the scaling transformations (4). Therefore, the equations $D_m^K(g_2, g_3) = 0$ can be rewritten as $C_m^K(J) = 0$, and these C_m^K are called *Cohn's polynomials*.

Corollary 1.2. *(Maier's conjecture)* $\deg C_m^I = \lfloor ((d_m^I)^2 - d_m^I + 4)/6 \rfloor$ *and* $\deg C_m^{II} = d_m^{II}(d_m^{II} - 1)/2$, *where $d_m^K = \deg_\lambda F_m^K$, as in (8), (9).*

Our second application, and the original motivation of this work is the problem of describing degeneration of metrics of constant positive curvature with conic singularities which recently attracted substantial attention,

[9, 10, 11, 14, 21, 22, 25, 26]. Let S be a compact surface, and $\alpha_1, \dots, \alpha_n$ positive numbers. Consider Riemannian metrics on S with n conic singularities with the angles $2\pi\alpha_j$. Each such metric defines a conformal structure on S with n marked points, so we have the forgetful map assigning this conformal structure to the metric. The goal is understanding the space of such metrics and the properties of the forgetful map.

In this paper we restrict ourselves to the case when S is a torus with one singularity with the angle $2\pi\alpha$, where $\alpha = 2m+1$ is an odd integer. Following [26] we denote the set of all such metrics by $\mathrm{Sph}_{1,1}(\alpha)$. One can embed $\mathrm{Sph}_{1,1}(\alpha)$ into Lame_m: the image of this embedding consists of those Lamé equations whose projective monodromy is *unitarizable* (that is conjugate to a subgroup of $PSU(2)$.)

We have the forgetful map $\mathrm{Sph}_{1,1}(\alpha) \to \mathbf{C}_J$ which assigns to each metric its conformal class. It is known that when $\alpha > 1$ is not an odd integer, this forgetful map is proper and surjective [26], and $\mathrm{Sph}_{1,1}(\alpha)$ is properly embedded in Lame_m.

This is not the case for odd integers α, the fact discovered in [22] (see also [4] for a shorter proof of the main result of [22]). As the conformal class varies, a spherical metric can degenerate.

Let us define the set $\mathrm{LW}_m \in \mathrm{Lame}_m$ consisting of all Lamé equations whose projective monodromy consists of collinear translations (by the periods of the integral (19) below). In Section 10 we show that

$$\partial\mathrm{Sph}_{1,1}(2m+1) \subset \mathrm{LW}_m.$$

It is very likely that in fact equality holds, but we do not address this in the present paper. Then we describe the set LW_m.

Theorem 1.3. *The set* LW_m *consists of* $m(m+1)/2$ *curves. Projections of these curves on* $\mathbf{C}_J$ *are smooth real analytic curves (images of intervals under analytic functions with non-vanishing derivatives).*

We propose to call projections of the curves LW_m to $\mathbf{C}_J$ Lin–Wang curves. They can be seen in the pictures in [22, 4] and our Figs. 12, 13 for $m = 1$; in [21, 11] and our Figs, 14, 15 for $m = 2$, and our Figs. 16–18 for $m = 3$. Large part of the papers [9], [10] and [21] is dedicated to analytic study of these curves for small m; here we propose a different, geometric description of them.

1.2 Description of the method

Our main tool in this paper is a new geometric interpretation of Lamé functions and their moduli space $\mathbf{L}_m$. Lamé functions correspond to what we call *translation structures* on tori with one conic singularity with the angle $2\pi(2m+1)$ and m simple poles. ("Simple pole" refers to the developing map; its differential has double poles).

Let (S, O) be an elliptic curve, that is S is a torus with a marked point $O \in S$, and $m \geq 0$ an integer. Translation structures we are talking about can be identified with Abelian differentials of the second kind $g(z)dz$ on S with single zero of multiplicity $2m$ at O, and m double poles, subject to the condition that *all residues vanish*. Two translation structures are *equivalent* if the differentials differ by a non-zero constant factor.

We refer to a survey [31] of translation structures. Structures considered in this survey have no poles and correspond to Abelian differentials of the first kind. To explain the name "translation structure", consider the Abelian integral

$$f(z) = \int_{z_0}^{z} g(\zeta)d\zeta. \tag{19}$$

This is a multi-valued function on S with a single critical point at O, and the monodromy of f consists of translations by the periods of the integral coming from the fundamental group of S. This function f is a developing map of a singular flat structure on S: it has one conic singularity with the angle $2\pi(2m+1)$ at O and m simple poles; the monodromy of this structure consists of translations, and the local monodromy at all points is trivial.

Proposition 1.1. *The correspondence $w \mapsto \Omega = dx/(uw^2)$ is a bijection between the space of Lamé functions and the space of triples (S, O, Ω), where S is a torus, $O \in S$ a point, and Ω is an Abelian differential on S, which is invariant with respect to the conformal involution, and has a single zero of multiplicity $2m$ and m double poles with vanishing residues. This bijection defines a biholomorphic map between $\mathbf{L}_m$ and the moduli space of Abelian differentials of considered type.*

One can pull back the *flat* metric on $\mathbf{C}$ via f and obtain a flat metric on the torus with one conic singularity at O with the angle $2\pi(2m+1)$ and m simple "poles". A *pole* of a flat metric is a point which has a punctured neighborhood isometric to $\{z \in \mathbf{C} : |z| > R\}$ with Euclidean metric, for some

$R > 0$. We call our torus equipped with this metric a *flat singular torus*. Two flat singular tori are considered *equivalent* if there is an orientation-preserving diffeomorphism between them multiplying the metric by a non-zero constant.

To study flat singular tori we cut each of them into two congruent flat singular triangles. *Congruent* means "related by an *orientation-preserving* isometry".

Definition 1.1. A *flat singular triangle (FT)* is a closed disk with three marked boundary points which are called *corners,* equipped with a flat metric with conic singularities at the corners and possibly simple poles inside the disk or on the open boundary arcs (*sides*) between adjacent corners, and such that the sides are geodesic. A side passing through a pole must be "unbroken" at this pole: in the chart $\{z \in \mathbf{C} : |z| > R\}$ it corresponds to two rays of the *the same* line.

Alternatively an FT can be described as a triple $(D, \{a_j\}, f)$, where D is a closed disk in the complex plane, (a_1, a_2, a_3) three distinct boundary points, and f a locally univalent meromorphic function on $D \backslash \{a_j\}$ with conic singularities at a_j, which means

$$f(z) = f(a_j) + (z - a_j)^{\alpha_j} h_j(z),$$

where $\alpha_j > 0$, and h_j is analytic near a_j, $h_j(a_j) \neq 0$, and such that the images of the sides $f([a_j, a_{j+1}]) \subset \ell_j \cup \{\infty\}$ where ℓ_j are three straight lines (not necessarily distinct) in the complex plane.

Two such triples $(D, \{a_j\}, f)$ and $(D', \{a'_j\}, g)$ are *equivalent* if there is a conformal[1] homeomorphism $\phi : D \to D'$, $\phi(a_j) = a'_j$, and complex constants c_1, c_2 such that $f = c_1 g \circ \phi + c_2$.

These two definitions of FT are equivalent: for a given triple, we pull back the Euclidean metric from $\mathbf{C}$ via f and obtain a metric on D satisfying the first definition. In the opposite direction, given such a metric we obtain f as its developing map.

It is easy to see that the sum of interior angles $\pi\alpha_j$ of a flat singular triangle is an odd integer multiple of π. If one angle is an integer multiple of π, then all three of them are integer multiples of π.

An FT can be visualized by making a picture of its image in the plane under the developing map f. Such a picture consists of three lines (not

[1]We assume that the complex plane has the standard orientation, and conformal maps preserve it otherwise we call them anti-conformal.

necessarily distinct), three (pairwise distinct) points of their intersections $f(a_j)$, and a marking of the angles. See Figs. 1a, 1b, 1d, 1e, 2a-f. We mark the angles by little arcs near the images of the corners, and write a_j instead of $f(a_j)$ in the pictures. Two such pictures define the same FT if they are related by a complex affine map.

An FT is called *balanced* if its angles $\pi\alpha_1, \pi\alpha_2, \pi\alpha_3$ satisfy the triangle inequalities

$$\alpha_i \leq \alpha_j + \alpha_k, \tag{20}$$

for all permutations of (i, j, k). For example, triangle with the angle sum π in Fig. 1a is balanced if and only if all its angles are $\leq \pi/2$. A triangle with the angle sum 3π in Fig. 1b is balanced if and only if the largest angle is $\leq 3\pi/2$.

All flat singular triangles whose angles are integer multiples of π are balanced. A balanced triangle is called *marginal* if we have equality in (20) for at least one permutation (i, j, k). Otherwise it is called *strictly balanced*.

We abbreviate the expression "balanced flat singular triangle" as BFT.

Our main technical result is the following

Theorem 1.4. *Every flat singular torus has a decomposition into two congruent BFT. When the triangles are strictly balanced, this decomposition is unique up to a cyclic permutation of the corner labels. If they are marginal, there are at most two such decompositions: a marginal triangle and its reflection define the same torus.*

This is similar to Theorem 1.3 in [14] for spherical tori with one singularity. Theorem 1.4 gives a parametrization of our moduli space $\mathbf{L}_m$ by a simpler moduli space $\mathbf{T}_m$ for BFT's with the sum of the angles $\pi(2m+1)$. This last space admits a nice partition into open cells which is used to prove Theorem 1.1.

The plan of the paper is the following. In section 2 we recall basic facts about Lamé equations and Lamé functions, and explain the connection between Lamé functions and translation structures.

In section 3 we discuss BFT and define a map $\Phi = \Phi_m : \mathbf{T}_m \to \mathbf{L}_m$. Explicit local coordinates on $\mathbf{T}_m$ are described in Section 4, and we show that Φ is complex analytic and proper. The proof of properness is based on the study of geodesics on flat singular tori.

In section 5 we prove the first part of Theorem 1.4, surjectivity of Φ.

In section 6 we develop a classification of BFT and explicitly describe a partition of $\mathbf{T}_m$ into open cells. We show that $\mathbf{T}_m$ consists of two connected components, and that Φ is in fact 3-to-1 on the subset of strictly balanced triangles, and 6-to-1 on the subset of marginal triangles. Factoring $\mathbf{T}_m$ by an appropriate equivalence relation we obtain a space $\mathbf{T}_m^*$ and show that the induced map $\Phi_m^* : \mathbf{T}_m^* \to \mathbf{L}_m$ is injective, thus completing the proof of Theorem 1.4.

In section 7 we analyze the natural partition of $\mathbf{T}_m$ and prove Theorem 1.1.

In section 8 we prove Theorem 1.2 and its two corollaries. This is based on Lemma 8.2 which is proved in Section 9.

The last two sections are devoted to spherical metrics: in Section 10 we discuss the monodromy of Lamé equations, and in Section 11 we produce equations and pictures of Lin–Wang curves, enumerate them, and show that they are smooth and real analytic.

Since we refer to some figures many times, in different places, all figures are collected at the end of the paper, after the reference list.

We thank Walter Bergweiler, Robert Maier and Vitaly Tarasov for useful discussions. Walter Bergweiler produced Figs. 12–18 and a Maple program generating polynomials F_m. Vitaly Tarasov proved Lemma 8.2. We also thank Eduardo Chavez Heredia for bringing [28] to our attention.

2 Lamé equations, Lamé functions and translation structures

We use the form (3) of the Lamé equation. Every solution W of (3) is meromorphic in the z-plane. Indeed, by the existence theorem for linear ODE, the singularities of solutions belong to the lattice Λ, and plugging a power series for $W(z)$ at 0 shows that there are two linearly independent meromorphic solutions.

Proof of Proposition 1.1.

We start with a Lamé function and assign to it a translation structure. Let W be a meromorphic solution of (3) whose square is even and Λ-periodic.

Then

$$W(z+\omega) = \pm W(z), \quad \omega \in \Lambda. \tag{21}$$

Now

$$W_1(z) := W(z) \int^z W^{-2}(\zeta) d\zeta \tag{22}$$

is another solution of (2), linearly independent of W, which can be seen by direct computation, so it must be also meromorphic, since every solution of (3) is meromorphic. It follows that all residues of $W^{-2}(\zeta)d\zeta$ vanish. Now the ratio of two solutions $f = W_1/W$ is an Abelian integral of the second kind, and as a ratio of two solutions of a second order linear equation, it also satisfies the Schwarz equation

$$\frac{f'''}{f'} - \frac{3}{2}\left(\frac{f''}{f'}\right)^2 = -2\left(m(m+1)\wp + \lambda\right),$$

thus all critical points of f are in Λ and f is $(2m+1)$-to-1 at these points.

So every Lamé function defines a translation structure. The differential $W^{-2}(z)dz$ descends via the map

$$z \mapsto (\wp(z), \wp'(z)) = (x, u),$$

to the differential $w^2(x)dx/u$ on the curve (1) as stated in Proposition 1.1. This differential is invariant with respect to the conformal involution of the elliptic curve, so its pull-back to the universal cover is even.

Conversely, suppose that a translation structure

$$f(z) = \int^z g(\zeta) d\zeta \tag{23}$$

is given. Then g is an even elliptic function with m double poles per period parallelogram, vanishing residues, and zeros of order $2m$ at the points of Λ. So $g = W^{-2}$ for some meromorphic function W satisfying (21). Now we define W_1 by (22), and a direct computation shows that

$$WW_1' - W'W_1 = 1.$$

This means that W and W_1 are two linearly independent solutions of some equation $W'' = PW$, where P is an elliptic function with periods Λ. As the only pole of P can occur at a critical point of f, we conclude that poles of

P must be at the points of Λ, and a simple calculation with power series at 0 shows that

$$P(z) = m(m+1)z^{-2} + O(1), \quad z \to 0,$$

so $P(z) = m(m+1)\wp(z) + \lambda$ with some $\lambda \in \mathbf{C}$, and thus W is a Lamé function.

We recall that two Lamé functions W_1 and W_2 are equivalent if $W_1(z) = cW_2(kz)$ for some c and k in $\mathbf{C}^*$. Translation structures are equivalent if their developing maps f_1, f_2 are related by post-composition with an affine map: $f_1(z) = af_2(kz) + b$, $a, k \in \mathbf{C}^*$, $b \in \mathbf{C}$.

We proved that *equivalence classes of degree m Lamé functions are in one-to-one correspondence with classes of translation structures on the torus with one conic singularity with the angle $2\pi(2m+1)$.*

It is clear that this correspondence is continuous and holomorphic, therefore it is biholomorphic. □

Let us recall how the polynomial F_m is computed (another method is described in Section 6). It is convenient to use the algebraic form of the Lamé equation (2) which can be also written as

$$w'' + \frac{1}{2}\left(\sum_{j=1}^{3} \frac{1}{\zeta - e_j}\right) w' = \frac{m(m+1)\zeta + \lambda}{4(\zeta - e_1)(\zeta - e_2)(\zeta - e_3)} w,$$

where $w = y \circ \wp$. Since the only singularities in $\mathbf{C}$ of equation (3) are e_j, and the local exponents at these singularities are $\{0, 1/2\}$, each Lamé function can be written as

$$w(\zeta) = c \prod_{j=1}^{3} (\zeta - e_j)^{k_j/2} \prod_{j=1}^{n} (\zeta - \zeta_j), \tag{24}$$

where $k_j \in \{0, 1\}$ and

$$\sum_{j=1}^{3} k_j + 2n = m. \tag{25}$$

Plugging $\zeta = \zeta_j$ into (3) we obtain after simple calculations (see, for example, [30, 23.21]) the following system of equations for ζ_j

$$2 \sum_{j:j\neq k}^{n} \frac{1}{\zeta_k - \zeta_j} + \sum_{j=1}^{3} \frac{k_j + 1/2}{\zeta_k - e_j}, \quad 1 \le k \le n. \tag{26}$$

This system of equations determines Lamé functions. According to a theorem of Heine and Stieltjes [30, 23.46], system (26) has at most $n+1$ solutions and exactly $n+1$ for generic e_j. Moreover, it has exactly $n+1$ solutions when all e_j are real. System (26) is a very special case of the Bethe ansatz equations which frequently occur in mathematical physics and in the study of metrics with conic singularities.

Lamé functions are classified according to the values of k_j in (24): traditionally the number

$$1 + \sum_{j=1}^{3} k_j \in \{1, 2, 3, 4\}$$

is called the *kind* of a Lamé function [30].

Using (25) and Stieltjes theorem we conclude that the total number of Lamé functions for a given generic lattice is $2m+1$, and this is the degree of the Lamé spectral polynomial F_m with respect to λ. The number of Lamé functions is exactly $2m+1 = d_m^I + d_m^{II}$ for lattices with real e_j, or equivalently with real g_j with $g_2^3 - 27g_3^2 > 0$.

It is easy to see that for even $m \geq 2$ there exist Lamé functions of the first and third kind, we define the corresponding subsets by $\mathbf{L}_m^I$ and $\mathbf{L}_m^{II}$. Similarly, when $m \geq 3$ is odd, we define $\mathbf{L}_m^I$ as the set of Lamé functions of the fourth kind, and $\mathbf{L}_m^{II}$ as the set of Lamé functions of the second kind. This explains why $\mathbf{L}_m$ has *at least two components* when $m \geq 2$. The more difficult result, which is a part of Theorem 1.1, is that these components are in fact irreducible.

Connection with spin structures.

Connected components of moduli spaces of Riemann surfaces endowed with nonzero holomorphic differentials were classified by Kontsevich and Zorich [18]; the case of meromorphic differentials was treated by Boissy [5]. A consequence of Theorem 4.1 in [5] is that the moduli space of triples (S, O, Ω), where (S, O) is an elliptic curve and Ω is a meromorphic differential on S with a zero at O of order $2m$ and m poles $q_1, \ldots, q_m$ of order 2 (and arbitrary residues), has exactly two connected components. Moreover, such components are distinguished by the *spin invariant* (already defined in [18, Sect. 2.2]). In our particular case, the spin invariant of (S, O, Ω) is *odd* if there exists a function on S with simple poles at $q_1, \ldots, q_m$ and a zero of order m at O, and it is *even* if such function does not exist.

Proposition 2.1. *A Lamé function w is in $\mathbf{L}_m^I$ if the spin invariant of the corresponding translation surface is odd, and w is in $\mathbf{L}_m^{II}$ if the spin invariant is even.*

Proof. Let (S, O, Ω) be the translation surface associated to the Lamé function w. In particular, $\Omega = \varphi/w^2$, where φ is a nonzero holomorphic differential on S, see Proposition 1.1 Then the spin invariant of (S, O, Ω) is odd if and only if w is a well-defined function on S, which happens if and only if $w = Q(x)$ or $w = Q(x)u$ for a suitable $Q \in \mathbb{C}[x]$. Hence, the spin invariant is odd if and only if w is of type I. □

As a consequence of [5, Thm. 4.1] we obtain

Corollary 2.1. *The space $\mathbf{L}_m$ of Lamé functions is the disjoint union of the subset $\mathbf{L}_m^I$ of Lamé functions of type I and of the subset $\mathbf{L}_m^{II}$ of Lamé functions of type II.*

The techniques of [5] do not allow to study connected components of moduli of meromorphic differentials with vanishing residues. So it does not follow from [5] that $\mathbf{L}_m$ has exactly two connected components, and so that $\mathbf{L}_m^I$ and $\mathbf{L}_m^{II}$ are connected.

3 Balanced flat singular triangles

In this section we consider balanced flat singular triangles (BFT) with marked corners a_1, a_2, a_3, enumerated according to the positive orientation of the boundary (counter-clockwise).

We denote the interior angles at these corners by $\pi\alpha_1, \pi\alpha_2, \pi\alpha_3$. As we already noticed, the sum of the angles is an odd multiple of π, more precisely

$$\alpha_1 + \alpha_2 + \alpha_3 = 4n + 2k + 1 = 2m + 1, \tag{27}$$

where n is the number of interior poles, and k is the number of boundary poles. To prove (27) we recall the argument used in the proof of the Schwarz–Christoffel formula. Consider the developing map f defined in the upper half-plane with corners at $(a_1, a_2, a_3) = (0, 1, \infty)$. Since the monodromy of f is affine, f''/f' must extend to the complex plane as a rational function whose poles are symmetric with respect to the real line, and we have

$$\frac{f''}{f'}(z) \sim \frac{\alpha_j - 1}{z - a_j}, \quad z \to a_j, \quad j \in \{1, 2\}, \quad \frac{f''}{f'}(z) \sim -\frac{\alpha_3 + 1}{z}, \quad z \to \infty,$$

and

$$\frac{f''}{f'}(z) \sim -\frac{2}{z - z_j}, \quad z \to z_j$$

at the poles. So (27) follows by the Residue Theorem.

Fig. 1a shows a triangle with $n = k = 0$. In Fig. 1b $n = 0, k = 1$. Fig. 1d shows a triangle with $n = 1, k = 0$ (left) and two triangles with $n = 0, k = 2$ (right). Fig. 1e shows three triangles with $n = 1, k = 0$. Fig. 2 shows all types of triangles with sum of the angles 5π ($m = 2$).

We also recall that *either none of the α_j or all of them are integers.*

Proposition 3.1. *An FT with non-integer α_j is completely determined by the angles, and any positive angles $\pi\alpha_j$ where α_j are not integers and their sum is odd can occur.*

For integer angles, the necessary and sufficient condition of existence of FT is that the sum of α_j is odd and (20) is satisfied. For any such angles, there are three one-parametric families of FT's.

A similar result for spherical triangles was proved in [12].

Proof. The first statement is essentially due to Klein [17]. If our triangle is modeled on the upper half-plane $D = \overline{H}$ with vertices $(a_1, a_2, a_3) = (0, 1, \infty)$ then the developing map $f : \overline{H} \to \overline{\mathbf{C}}$ satisfies the Schwarz equation with three singularities $(0, 1, \infty)$ and α_j determine this equation completely. When the α_j are not integers, the monodromy representation corresponding to this equation is non-trivial, and there is only one choice, up to an affine transformation, of a solution with affine monodromy.

If all α_j are integers, then the monodromy representation is trivial, and the developing map f extends from its domain D to the whole Riemann sphere and we obtain a rational function with three critical points a_1, a_2 and a_3. The images of all three sides under the developing map f belong the same line ℓ. Preimage $f^{-1}(\ell) \cap \overline{D}$ is called the *net* of f (see [13]). The net is a cell decomposition of D with three vertices a_1, a_2, a_3. The 1-cells of this decomposition are disjoint chords of the disk D and three arcs of ∂D. The number of chords in the interior of D which are adjacent to a_j is $\alpha_j - 1 \geq 0$. If m_j is the number of chords from a_i to a_k, then $\alpha_j - 1 = m_i + m_k$, and these three equations have unique non-negative solution (m_1, m_2, m_3) if and only if the integers $\alpha_j \geq 1$ satisfy (20) and their sum is odd. Thus the angles determine the net. Once the net is given, the developing map can be recovered from the values $f(a_1), f(a_2), f(a_3)$ which in the considered case

belong to a line. It is clear that one of the 2-faces of a net is a triangle while the others are digons. Suppose that the triangular face is mapped by f onto the upper half-plane. Then we have three possible orderings of $f(a_j)$ on the real line. By scaling we may arrange that $\min_j f(a_j) = 0$ and $\max_j f(a_j) = 1$, then the intermediate point of the three $f(a_j)$ serves as a parameter. So the set of triangles with given integer angles is parametrized by three intervals. □

Examples of nets of triangles are shown in Fig. 1c, where the stars mark the location of the poles of f. These three nets correspond to triangles with the angles $(2\pi, 3\pi, 4\pi)$. In Fig. 1d, three triangles with the angles $(\pi, 2\pi, 2\pi)$ are shown together with their nets.

Let us define two types of triangles which we call *primitive*. A primitive triangle of type A has all angles in $(0, \pi)$ and their sum is π (Fig. 1a), and the primitive triangle of type B has one angle in $([\pi, 2\pi)$, two others in $(0, \pi]$, and the sum of the angles is 3π (Fig. 1b).

Proposition 3.2. *Every BFT can be obtained from one of the two primitive triangles A or B by gluing half-planes to the sides.*

Proof. This is essentially due to Klein [17], but we sketch a proof. Consider the case of non-integer angles. Let $\alpha_i = \{\alpha_i\} + \lfloor \alpha_i \rfloor$, be the decomposition into fractional and integer parts.

a) If $\sum \lfloor \alpha_i \rfloor$ is even, then $\sum \{\alpha_i\}$ is odd. Since the last sum belongs to $(0, 3)$, we must have

$$\sum \{\alpha_i\} = 1. \tag{28}$$

Since our triangle is balanced, and we have (28), we obtain for all permutations (i, j, k) of $(1, 2, 3)$:

$$\begin{aligned} \lfloor \alpha_i \rfloor &= \alpha_i - \{\alpha_i\} \le \alpha_j + \alpha_k - \{\alpha_i\} = \lfloor \alpha_j \rfloor + \lfloor \alpha_k \rfloor + \{\alpha_j\} + \{\alpha_k\} - \{\alpha_i\} \\ &< \lfloor \alpha_j \rfloor + \lfloor \alpha_k \rfloor + 1. \end{aligned}$$

So $\lfloor \alpha_i \rfloor \le \lfloor \alpha_j \rfloor + \lfloor \alpha_k \rfloor$. It follows that the following quantities are non-negative integers:

$$x_i = (\lfloor \alpha_j \rfloor + \lfloor \alpha_k \rfloor - \lfloor \alpha_i \rfloor)/2,$$

and we have $\lfloor \alpha_i \rfloor = x_j + x_k$, for all permutations (i, j, k) of $(1, 2, 3)$. So we can take a triangle with the angles $\{\alpha_j\}$ of the type A and glue x_j half-planes

to the side opposite to a_j, for each j. The resulting triangle has the same angles as our original triangle, so it is the same triangle by Proposition 3.1.

b) If $\sum\lfloor\alpha_i\rfloor$ is odd, then we decrease one of the integer parts (for example, the largest one) by 1, and increase the corresponding fractional part by 1. So we set for some i

$$p_i = \lfloor\alpha_i\rfloor - 1, \quad \alpha_i' = \{\alpha_i\} + 1,$$

leaving other numbers unchanged ($\alpha_j' = \{\alpha_j\},\ p_j = \lfloor\alpha_j\rfloor$, and similarly for k). Now we have

$$\alpha_i' \in (1,2), \quad \alpha_j' \in (0,1), \quad \alpha_k' \in (0,1), \tag{29}$$

and since $\sum\{\alpha_\ell\}$ is even and less than 3 in this case, it must be 2, and thus

$$\sum \alpha_\ell' = 3. \tag{30}$$

Now, since our triangle is balanced, and using (30) and (29) we obtain

$$p_i = \alpha_i - \alpha_i' \le \alpha_j + \alpha_k - \alpha_i' = p_j + p_k + \alpha_j' + \alpha_k' - \alpha_i' \le p_j + p_k + 1,$$

and since the sum of p_ℓ is even, we conclude that $p_i \le p_j + p_k$. So we can define x_i, x_j, x_k as in part a) and conclude that our triangle is obtained from a triangle with the angles α_ℓ' of the type B, by gluing x_ℓ half-planes to the side opposite to a_ℓ.

Triangles with integer angles can be considered using their nets introduced in the proof of Proposition 3.1. A net is a chord diagram in a disk with three vertices on the circle. Evidently each net has one triangular face, and the rest of the faces are digons. Triangular face corresponds to the primitive triangle and digons are half-planes. Since the angle sum is odd, only case b) can occur, and the primitive triangle is of type B with the angles (π,π,π). Thus the primitive triangle in this case is just a half-plane with three marked boundary points. □

Corollary 3.1. *Each side of a BFT contains at most one pole, and the developing map sends each side (a_i, a_{i+1}) injectively either to the interval $(f(a_i), f(a_{i+1}))$, or to the complement of this interval on the line in $\mathbf{C}\cup\{\infty\}$ containing it.* □

Remarks. 1. By analyzing the proof of Proposition 3.2 one can obtain the following criterion: the side opposite to a_i contains a pole if and only if

$$\lceil (\lfloor \alpha_j \rfloor + \lfloor \alpha_k \rfloor - \lfloor \alpha_i \rfloor - 1)/2 \rceil \quad \text{is odd.}$$

2. It follows from this Corollary and from (27) that for each $m \geq 2$ we have exactly two possibilities for the number of sides with a pole. When m is even, we have either none or 2 sides with poles. If m is odd, we have ether one or three sides with poles. This shows that the set $\mathbf{T}_m$ of all BFT's with the angle sum $\pi(2m+1),\ m \geq 2$ must have at least four connected components. We show in Section 6 that there are exactly four.

3. The decomposition into a primitive triangle and half-planes stated in Proposition 3.2 is canonical when $\sum \lfloor \alpha_j \rfloor$ is even, but not canonical when it is odd. In the latter case, we can obtain from one to three such different decompositions, depending on the number of positive $\lfloor \alpha_j \rfloor$.

4. The primitive triangle T' obtained from a balanced triangle T may be unbalanced. In this case, there is always at least one half-plane in T glued to the side of T' which is opposite to the largest andgle of T'. Indeed, let α'_j be the angles of T', and α_1 is the largest one. Then the angles of T are $\alpha_i = \alpha'_i + x_j + x_k$, where (i, j, k) is a permutation of $(1, 2, 3)$, and x_j are the numbers of half-planes glued to the sides opposite to α'_j, $j = 1, 2, 3$. Since T is balanced,

$$\alpha'_1 + x_2 + x_3 = \alpha_1 \leq \alpha_2 + \alpha_3 = \alpha'_2 + \alpha'_3 + x_2 + x_3 + 2x_1,$$

so $\alpha'_1 = \alpha'_2 + \alpha'_3 + 2x_1$. Thus if T' is unbalanced, we have $x_1 > 0$.

Construction of the map Φ.

Let $\mathbf{T}_m$ be the set of all balanced triangles with the sum of the angles $\pi(2m+1)$. For every $T \in \mathbf{T}_m$ we define a singular flat torus $\Phi(T)$ in the following way. We take two copies of T and identify each pair of corresponding sides by the *orientation-reversing* isometry.

Thus all corners of both copies are glued into one point, and the sides are glued into three simple loops on the torus based at this point and otherwise disjoint.

Notice that the resulting torus has an orientation-preserving isometric involution which interchanges the two triangles. The four fixed points of this

involution are: the conic singularity (corresponding to the vertices of the triangle) and the "midpoints of the sides" which are points of order 2 on the elliptic curve. If a side is unbounded, its midpoint is a pole.

With such gluing we obtain a flat singular torus with one singularity with the angle $2\pi(2m+1)$. There are m simple poles on the torus coming from the poles of the metric on the triangle. An interior pole of T gives two poles on $\Phi(T)$, while a pole on a side of T gives one pole on $\Phi(T)$. This gives another, geometric proof of (27).

Let T be a BFT with corners a_1, a_2, a_3 and developing map f. Let $b_j = (f(a_i)+f(a_k))/2$, where (i,j,k) is a permutation of $(1,2,3)$. We define affine maps s_j to be rotations by π about b_j. Consider the group generated by s_1, s_2, s_3. It contains a subgroup G consisting of translations; elements of G are products of even numbers of s_j. The following proposition is evident:

Proposition 3.3. *The monodromy group of the developing map of the flat singular torus $\Phi(T)$ is G.* □

In particular, the monodromy consists of collinear translations if and only if the angles of the triangle are integer multiples of π.

Next we address the question when two different BFT's can give the same (isometric up to a constant factor) tori. This can happen in at least two ways:

1. The triangles are obtained by a cyclic permutation of the corners.
2. Some pairs of marginal triangles define the same torus.

More precisely, we have

Proposition 3.4. *For a marginal triangle T with the angles $(\alpha_1, \alpha_2, \alpha_3)$ where $\alpha_1 = \alpha_2 + \alpha_3$, and the triangle T^* with the angles $(\alpha_1, \alpha_3, \alpha_2)$ the tori $\Phi(T)$ and $\Phi(T^*)$ are congruent.*

T and T^* are related by a reflection, an orientation-reversing isometry.

Proof of Proposition 3.4. First we notice that a marginal triangle cannot have integer angles (since the angle sum is odd), so it is completely determined by the angles. We use Klein's decomposition described in the proof of Proposition 3.2. Our triangle is obtained from a primitive triangle by gluing half-planes to the sides.

We claim that for a marginal triangle, no half-planes are glued to the side opposite to the larger angle. Indeed, let α'_j be the angles of the primitive

triangle, and $\alpha_j = \alpha'_j + p_j = \alpha'_j + x_i + x_k$, where p_j, x_i, x_k are non-negative integers, Then $\alpha_1 = \alpha_2 + \alpha_3$ implies

$$\alpha'_1 = \alpha'_2 + \alpha'_3 + 2x_1, \tag{31}$$

and we obtain that $x_1 = 0$ since $\alpha_1 < 2,\ a'_2 > 0, \alpha'_3 > 0$. This proves the claim.

We also conclude from (31) with $x_1 = 0$ that the primitive triangle T' with the angles $\alpha'_1, \alpha'_2, \alpha'_3$ corresponding to our triangle T is also marginal, with the larger angle α_1. If T' is of the type A, then $\alpha'_1 = 1/2$. If T' is of the type B, then $\alpha'_1 = 3\pi/2$. Gluing together two copies of T' along the side (a_3, a_1) we obtain either a rectangle in the plane, or a complement of a rectangle on the Riemann sphere. It is clear that rectangles obtained from T and T^* are congruent, and the corresponding tori $\Phi(T)$ and $\Phi(T^*)$ are also congruent, see Fig. 3. □

We give two examples illustrating Theorem 1.4 in the simplest cases.

Example 1. Consider a triangle T shown in Fig. 1a, whose angle sum is π. It is balanced iff all angles are at most $\pi/2$. Gluing two congruent copies of such a triangle along a common side, we obtain a parallelogram in the plane. Identifying the opposite sides of this parallelogram by translations we obtain a flat non-singular torus $\Phi(T)$ $(m = 0)$.

Now consider a flat non-singular torus L with a marked point O. Let $f : \mathbf{C} \to L,\ f(0) = O$ be the universal cover. Then there is a lattice $\Lambda \subset \mathbf{C}$ such that $L = \mathbf{C}/\Lambda$. A fundamental region D of this lattice can be taken in the form of a parallelogram which can be normalized so that the shorter side is $[0, 1]$. Let $[0, \tau]$ be the longer side. It is well known that τ can be always chosen in the fundamental region of the modular group

$$G = \{\tau : |\tau| \geq 1, |\mathrm{Re}\,\tau| \leq 1/2\}.$$

To achieve this one can normalize so that the shortest non-zero element of Λ is 1, then the shortest non-real element of Λ is τ. For $\tau \in G$, each diagonal of D breaks D into a pair of congruent triangles, such that at least one pair consists of balanced triangles. Both pairs consists of balanced triangles if and only if D is a rectangle, in which case the triangles of different pairs are marginal and are reflections of each other. It is easy to see that at least one diagonal breaks D into balanced triangles if and only if $\tau \in G$. This proves

Theorem 1.4 for $m = 0$. The proof in the general case is a generalization of this argument. $\square$

Example 2. Consider a triangle T in Fig. 1b. The angle sum is 3π ($m = 1$). Rotating T by π about the point $(a_1+a_3)/2$ we obtain a congruent triangle T'. Gluing T and T' along the side which contains pole, we obtain the "exterior parallelogram" Q. Identifying the opposite sides of Q by translations, we obtain the flat singular torus $\Phi(T)$ with the angle 6π at the singularity. It will be proved later that every flat singular torus with the angle 6π can be obtained from an exterior parallelogram by identifying the opposite sides by translations. We claim that every exterior parallelogram Q can be obtained by gluing two *balanced* triangles of the type B. Indeed, consider the diagonals of the parallelogram $\mathbf{C}\backslash Q$, and extend them to Q. Each extension of a diagonal breaks Q into two triangles of the type B, and it is easy to see that only for one diagonal these triangles are balanced, unless our Q is an exterior rectangle as in Fig. 3. When Q is an exterior rectangle, our triangles are marginal, and they are related by reflection as in Proposition 3.4. $\square$

Now we define an *equivalence relation* $\sim$ on $\mathbf{T}_m$, in accordance with statements 1, 2 before Proposition 3.4. Two BFT's T and T' are equivalent if either there is a congruence between them cyclically permuting the corners, or if they are marginal and related by a reflection as described Proposition 3.4. Then our map Φ is well defined on the equivalence classes, and we prove in Section 5 that the induced map

$$\Phi^*_m : \mathbf{T}^*_m \longrightarrow \mathbf{L}_m, \quad \mathbf{T}^*_m = \mathbf{T}_m/\sim$$

is bijective. We denote by Φ^* the map defined by this formula on the disjoint union $\mathbf{T}^*$ of $\mathbf{T}^*_m$, $m \geq 0$, and mapping it to the disjoint union $\mathbf{L}$ of $\mathbf{L}_m$.

4 Complex analytic coordinates on $\mathbf{T}_m$

We introduce a complex analytic structure on the set of BFT. We define functions on the set of BFT:

$$\phi_{i,j,k} = \frac{f(a_i) - f(a_j)}{f(a_k) - f(a_j)}.$$

All these functions are defined in a neighborhood of any triangle with non-integer α_j. For a triangle with integer α_j at least one such function is defined.

These functions are locally injective and we use them as complex coordinates on $\mathbf{T}^*_m$. The correspondence maps between charts are linear-fractional. So they define a complex analytic structure on $\mathbf{T}^*_m$ (and even a projective structure).

To show that the map Φ^*_m is complex analytic, we recall Proposition 3.3 which implies that $\phi_{i,j,k}$ are ratios of periods of the differential in Proposition 1.1. It is clear that periods and their ratios are analytic on $\mathbf{L}_m$ (which can be identified with a space of proportionality classes of differentials). We refer to a much more general statement of this kind in [2, Corollary 2.3].

So $\phi_{i,j,k}$ are local complex analytic coordinates on $\mathbf{T}^*_m$, and we have

Proposition 4.1. *The map $\Phi^*_m : \mathbf{T}^*_m \to \mathbf{L}_m$ is complex analytic.* □

Next we prove

Proposition 4.2. *The maps Φ^*_m are proper.*

Proof. We are going to show that a degenerating sequence of triangles gives a degenerating sequence of tori. First we clarify the notions of degenerating sequences.

For every flat singular torus L with one conic singularity at O, we define the set G of all simple geodesics loops based at O. Some of these loops may pass through a pole and thus have infinite length. The *systole* s_1 is the minimal length of all elements of G. The *second systole* $s_2 \geq s_1$ is the minimal length of all elements on G whose homotopy class is not a multiple of the class of some element of G of length s_1. Since we identify tori with proportional metrics, only the ratio s_2/s_1 is defined as a function on $\mathbf{L}_m$. It is clear that s_2/s_1 is bounded on every compact subset of $\mathbf{L}_m$.

If $s_2/s_1 \to \infty$ for a sequence of tori in $\mathbf{L}_m$, then this sequence diverges in $\mathbf{L}_m$, and we say that tori of this sequence degenerate.

Proposition 3.2 defines for every balanced T a primitive triangle T' which is of type A or B (Fig. 1a,b). When the sum of $\lfloor \alpha_j \rfloor$ is even, then T' is of type A and it is defined uniquely. When this sum is odd, we may have up to three choices for T'; they are of type B (see Remark 3 after Corollary 3.1). We pick one of them, as we did in the proof of Proposition 3.2.

This primitive triangle T' may be unbalanced. If this is the case, then there is at least one half-plane in T attached to the side of T' opposite to the largest angle of T' (Remark 4 after Corollary 3.1). Then we denote by T'' the union (more precisely the result of gluing) of T' with this half-plane.

When T' is balanced we set $T'' = T'$. We call T'' the *balanced extension* of T'. There are 4 types of T'': balanced of type A or B and balanced extensions of unbalanced A and B. We call these last two types A'' and B''.

The numbers $|f(a_i) - f(a_j)|$ are all the same for T, T' and T''. Consider the ratios

$$\frac{f(a_i) - f(a_j)}{f(a_k) - f(a_j)}$$

It is easy to see that if a sequence of triangles in $\mathbf{T}_m$ leaves every compact in $\mathbf{T}_m$ then one of these ratios tends to infinity. We call triangles of such a sequence *degenerate*, and notice that T, T' *and* T'' *degenerate simultaneously.* (Unbalanced triangle of type A can degenerate in a different way: when a vertex tends to an interior point of the opposite side. But its balanced extension does not degenerate in this case.)

We claim that s_1, s_2 for $\Phi(T'')$ are the same as for $\Phi(T)$. Indeed, attaching n half-planes to a side of a triangle T'' results in attaching a digon D (with poles) with angle $2\pi n$ at the two corners to the torus $\Phi(T)$. Every curve in such a digon with endpoints at ∂D is at least as long as the segment between its endpoints. On the other hand, there are four types of T'' of which A and B'' have all sides bounded, while the complementary segment of the unbounded side of A'' or B is at least s_2 for T''.

It remains to consider the tori $\Phi(T'')$, and to show that when T'' degenerates then $s_2/s_1 \to \infty$ for these tori. There are 4 cases to consider:

a) T' is balanced, then $T'' = T'$. Then T' is of type A or B, and balanced, and this is essentially the cases of Examples 1, 2 in the end of Section 3.

b) T' is unbalanced, T'' is the balanced extension of T' of the type A or B. One has to find the first and second systole of such tori $\Phi(T'')$.

We denote A'' and B'' the classes of triangles consisting of balanced extensions of unbalanced triangles of type A and B.

We are interested in the length spectrum of the set of geodesic loops in $\Phi(T_1)$ where T_1 is a balanced triangle of one of the types A, B, A'', B''. To find it we describe all geodesic loops of finite length in G for each type.

Lemma 4.1. *For T_1 of type A, all elements of G have finite length, and they are in bijective correspondence with indivisible elements*[2] *of the lattice*

[2]An element of $\mathbf{Z}^2$ is called indivisible if it is not an integer multiple of any other

generated by the sides of T_1. So s_1 and s_2 are the smallest and the second smallest lengths of sides of T_1.

For T_1 of type B, there are two elements in G of finite length. They correspond to the two sides of T_1 of finite length.

For T_1 type A'', let a_3 be the corner opposite to the side of infinite length, and denote $a = f(a_2) - f(a_1)$, $b = f(a_3) - f(a_1)$ Then the length spectrum is

$$\{|na + b| : n \in \mathbf{Z}\} \tag{32}$$

and $\{s_1, s_2\} = \{|b|, |a - b|\}$.

For T_1 of type B'', there are exactly three elements of G of finite length. They correspond to the sides of T_1.

Proof. We look at all geodesics starting at a vertex of T_1 with all possible slopes.

If T_1 is of type A, then the torus $\Phi(T_1)$ is a flat non-singular torus from Example 1 in Section 3. Elements of G are in bijective correspondence with segments whose endpoints are elements of the lattice and which contain no lattice points in their interiors.

For T_1 of type B, the torus $\Phi(T_1)$ can be represented as an exterior parallelogram Q whose opposite sides are identified by translations. Any geodesic starting from a vertex which is not a side of Q, visits the pole and thus has infinite length. The set G contains two elements of finite length (corresponding to two pairs of parallel sides of Q).

Let T_1 be the balanced extension of an unbalanced triangle T_2 with angle sum π, and f the developing map of T_1. We normalize so that $f(T_2) = (0, 1, b)$, so that $a = 1$, and $|b| \leq 1$. The torus $\Phi(T_1'')$ is partitioned into two triangles congruent to T_2 and two half-planes. Suppose that a geodesic starting from a vertex v is not a side of T_2. Then it visits the regions of our partition, one after another. Once the geodesic enters a half-plane it must stay there until it hits a pole, so the length of such geodesic is infinite. A geodesic in G of finite length must cross the two finite sides of T_1 alternatively, and its length is given by (32). See Fig. 4, which shows the images under the developing map: $f(T_1)$ is dark, the image of one congruent copy of $f(T_1)$ is grey, and images other congruent copies of T_2 are white triangles. Images of several geodesics issued from one corner are shown: the dotted lines are images of geodesics of infinite length which contain poles, and dashed lines

element.

are images of some geodesics in G of finite length. Since $|b| \leq 1$, the smallest and the second smallest elements of (32) are $|b|$ and $|1-b|$.

Now consider a torus $\Phi(T_1)$ where T_1 is of type B'', that is T_1 is a balanced extension of some unbalanced T_2 of type B. Then T_1 is an exterior triangle (exterior of a bounded triangle with angle sum π). Torus $\Phi(T_1)$ is obtained by gluing two copies of exterior triangles T_1. Every geodesic on this torus which does not correspond to a side of B'' passes through a pole. $\square$

We conclude from Lemma 4.1:

For a balanced triangle T, the first and second systoles of $\Phi(T)$ are two of the three numbers $|f(a_i) - f(a_j)|$.

It follows that when a balanced triangle T degenerates, then the torus $\Phi(T)$ also degenerates, therefore the map Φ is proper, and thus Φ^* is proper as well. This completes the proof of Proposition 4.2. $\square$

5 Surjectivity of Φ^*

We recall that $\mathbf{T}_m$ is the set of BFT with the angle sum $\pi(2m+1)$, and $\mathbf{T}^*_m = \mathbf{T}_m/\sim$ is the quotient by the following equivalence relation:

(i) we identify triangles obtained from each other by a cyclic permutation of the three vertices, and

(ii) we identify pairs of triangles described in Proposition 3.4.

In this section we prove that the map $\Phi^*_m : \mathbf{T}^*_m \to \mathbf{L}_m$ is surjective establishing the first part of Theorem 1.4. Injectivity will be proved in Section 6.

Proof of Surjectivity of Φ^*.

The plan of the proof is the following: for a given flat singular torus L we find two special geodesic loops whose complement is a quadrilateral Q. Then we construct cell decompositions C_2, C_4 of Q, and reassembling certain cells of C_4 we obtain a decomposition of L into two congruent balanced triangles.

Let L be a torus with the singular point O. Consider a germ at O of developing map $f : L \to \overline{\mathbf{C}}$, $f(O) = 0$. Let $g : \mathbf{C} \to L$ be a universal covering with $g(0) = O$. Then the composition[3]

$$F = f \circ g$$

[3]Many authors call this F a developing map.

has a meromorphic continuation to the whole plane. This meromorphic function satisfies

$$F(z+\omega) = F(z) + \eta, \quad \omega \in \Lambda. \tag{33}$$

Here $\omega \mapsto \eta(\omega)$ is a group homomorphism $\Lambda \to \mathbf{C}$, and there are two possibilities:

a) Generic case. The image of Λ is another lattice $\Lambda' \subset \mathbf{C}$, of rank 2, and $F : \Lambda \to \Lambda'$ is an isomorphism, or

b) Degenerate case. The image of Λ belongs to a line through the origin.

The pull back the flat metric via F has the length element

$$ds = |F'(z)||dz|.$$

This metric has conic singularities at the critical points of F which are the points of Λ, and some poles.

Let γ_1 be a shortest curve among all curves from 0 to some point $\omega \in \Lambda\backslash\{0\}$. We denote its endpoint other than 0 by ω_1. It is clear that γ_1 is a simple curve; $F(\gamma_1)$ is a segment $[0, \eta_1]$, where $\eta_1 \in \Lambda'\backslash\{0\}$, and the map $F : \gamma_1 \to [0, \eta_1]$ is a homeomorphism.

Let γ_2 be a shortest of all curves from 0 to some point $\omega_2 \in \Lambda\backslash\{\mathbf{Z}\omega_1\}$. The following lemma implies that γ_1 and γ_2 are disjoint except their common endpoint at 0.

Lemma 5.1. *The curves $g(\gamma_1)$ and $g(\gamma_2)$ in L intersect only at O.*

Proof. Suppose that this is not so, and let $p \neq O$ be a point of intersection. Since p is not a conic singularity, and our curves are geodesic, they must make a non-zero angle st p. It follows that the ratio of the periods of the differential df over $g(\gamma_1)$ and $g(\gamma_2)$ is not real.

Now we construct a loop Γ in L based at O which is shorter than $g(\gamma_2)$ and whose homology class is not a multiple of $g(\gamma_1)$. The point p breaks $g(\gamma_1)$ into two arcs, and we denote the shorter of these arcs by I_1. Similarly I_2 is the shorter of the two arcs into which p breaks $g(\gamma_2)$. Let Γ be the concatenation of I_1 and I_2. From our observations on the periods of df we conclude that

$$\int_\Gamma df \neq 0,$$

therefore Γ is non-trivial. Here we used that df has no residues at the poles. Moreover, this integral cannot be a real multiple of the integral over $g(\gamma_1)$,

so Γ is not a multiple of $g(\gamma_1)$. Finally, the length of Γ is at most the length of $g(\gamma_2)$, but Γ can be shortened since it has a non-zero angle at p, so we obtain a contradiction. $\square$

The loops $g(\gamma_1)$ and $g(\gamma_2)$ cut the torus into a quadrilateral. Preimage of this quadrilateral under g is a quadrilateral in the plane bounded by γ_1, γ_2 and their shifts $\gamma_1 + \omega_2$ and $\gamma_2 + \omega_1$. From Lemma 5.1 we conclude that all four curves are pairwise disjoint except their endpoints.

Thus we obtain a Jordan quadrilateral that will be called Q (the boundary is included).

Since the curves $g(\gamma_1)$ and $g(\gamma_2)$ have intersection index ± 1, they generate the fundamental group of the torus, and it follows that Q does not contain other lattice points except $0, \omega_1, \omega_2$ and $\omega_1 + \omega_2$. The image $F(\partial Q)$ consists of 4 straight segments which form a parallelogram in the plane in the non-degenerate case. In the degenerate case these 4 segments belong to the same line. Next we study

Topology of the map $F : Q \to \overline{\mathbf{C}}$.

The following argument is purely topological, so we consider an arbitrary Jordan quadrilateral Q in the plane (a closed disk with four distinct marked boundary points $a_1, \ldots, a_4$, which we call *corners*, enumerated according to the standard orientation). The boundary arcs (a_i, a_{i+1}), where i is a residue modulo 4, are called the *sides*.

Let $F : Q \to \overline{\mathbf{C}}$ be a continuous function which is a local homeomorphism on the complement of the corners, and topologically holomorphic[4] at the corners.

About the boundary behavior we make one of the two assumptions:

a) Generic case: $F(\partial Q)$ is a Jordan curve γ and $F : \partial Q \to \gamma$ is a homeomorphism, or

b) Degenerate case: the restrictions of F to the sides are homeomorphisms onto the image of each side, and these images are segments of the same straight line ℓ in $\mathbf{C}$. The images of opposite sides have equal length.

We want to obtain a topological description of possible partitions of Q by $F^{-1}(\gamma)$ in case a) and by $F^{-1}(\ell)$ in case b).

First we address the generic case a). Consider the cell decomposition C_1

[4]Topologically equivalent to $z \mapsto z^{n_i}$, $1 \le i \le 4$.

of the Riemann sphere which has two 2-cells: the interior I and the exterior E of γ (Fig. 5d). The 0-cells are $F(a_j)$ and 1-cells are the four arcs into which $F(a_j)$ divide γ. We assign the labels to 0- and 1-cells by the following rules: $F(a_j)$ has label j; the arc $(F(a_j), F(a_{j+1}))$ has label j.

Now consider the preimage $C_2 = F^{-1}(C_1)$ in Q. Our assumptions about F imply that C_2 is a finite cell decomposition of Q. It is called the *net* of F. Closures of the cells of C_2 are mapped onto the closures of the cells of C_1 homeomorphically, and we label cells of C_2 by their images. Since F is a local homeomorphism on $Q\backslash\{a_j\}$, the 1-skeleton of C_2 consists of simple curves which can meet only at the corners. We call the intersections of these curves with the interior of Q *arcs* and define the length of an arc as the number of 1-cells that it contains. An example of the cell decomposition C_2 is shown in Fig. 5a, where the black dots are 0-cells.

The faces of C_2 are quadrilaterals, and we classify them as follows:

A face is called *lateral* if its boundary consists of one arc of length 1 and one arc of length 3, both arcs having as endpoints two adjacent corners of Q.

A face is called *diagonal* if its boundary consists of two arcs of length 2 both having as endpoints two opposite corners of Q.

A face is called *triangular* if its boundary consists of two arcs of length 1 and one arc of length 2, arcs of length 1 connecting pairs of adjacent corners, while the arc of length 2 connects opposite corners.

A face is called *quadrilateral* if its boundary consists of 4 arcs of length 1, each connecting a pair of adjacent corners of Q.

Fig. 5a contains 8 lateral, 1 diagonal and 2 triangular faces.

Let us show that this classification exhausts all possibilities for the faces of C_2. A face of C_2 cannot have all 4 boundary vertices in the interior of Q, since then there would be an adjacent face which is not simply connected. Neither a face of C_2 can have two vertices at the same corner, because the restriction of f on the boundary of a face is a homeomorphism onto γ. A face of C_2 cannot have only one vertex at a corner, because if this were the case, an adjacent 2-cell will have all its 4 boundary edges the same as the original face, which is impossible.

Lemma 5.2. *Under the assumption a) there are the following possibilities:*

(i) The net contains one quadrilateral face and some (possibly none) lateral faces.

(ii) The net contains at least one diagonal face, two triangular faces and several (possibly none) lateral faces. All diagonal faces share the same oppo-

site corners on their boundaries.

This lemma and its proof are illustrated in Fig. 5. In Fig. 5b case (i) is illustrated (C_2 is shown with bold lines). Fig. 5a is an example of case (ii).

Proof. Notice that lateral faces come in pairs, so the number of lateral faces sharing two given corners a_i, a_{i+1} on their boundaries must be even. So the innermost arc in Q, connecting (a_i, a_{i+1}), has length 1. Removing all lateral faces, we obtain a smaller quadrilateral Q', and a cell decomposition C_3 of it which has no lateral faces. The restriction of f to Q' satisfies the same conditions as f on Q: the boundary ∂Q is mapped onto γ homeomorphically.

If C_3 consists of a single face, we are in case (i). If C_3 contains a diagonal face, suppose it has a_1 and a_3 on the boundary. Then all diagonal faces must have a_1 and a_3 on their boundaries. Removing all of them, we obtain two triangular faces, so we are in case (ii).

If C_2 contains no diagonal faces, then there are no triangular faces. Indeed, suppose that the cell decomposition of Q' consists of just two triangles. The 1-cells on the boundary of each triangle have 4 distinct labels, and two of these 1-cells are in the common boundary of these two triangles. But the 1-cells on the boundary of Q' also have 4 distinct labels, and this is evidently impossible. Thus if there are no diagonal faces in Q', then there are also no triangular faces, and we are in case (i). □

Transformation of the cell decomposition C_2 into another cell decomposition C_4 of Q.

The edges of C_4 are defined as follows. First, they are arcs of length 1 of C_2. Then we discard all arcs of length at least 2, and add new edges by the following rules:

Suppose that C_2 has a diagonal face G. We recall that cells of C_2 are labeled by their images in C_1. If G is a cell of C_2 is labeled I, we draw the *diagonal*: the F-preimage in G of that diagonal of the parallelogram I which has two corners of Q as its extremities. If G is labeled E, we use one of the two *exterior diagonals* of the parallelogram I. An exterior diagonal is the complement to a diagonal in the line which contains this diagonal. In Fig. 5b the added diagonal is red (dotted), and the discarded arcs are grey.

If C_2 has no diagonal faces, then it has one quadrilateral face. If this quadrilateral face is labeled I, we break this quadrilateral face by the preimage of the *shorter* diagonal of the parallelogram I. If the quadrilateral face of C_2 is labeled E we break this quadrilateral face by the preimage of the

exterior diagonal of I which connects the two vertices of this parallelogram with the larger exterior corner (Fig. 5g). Partition of a quadrilateral face is shown if Fig. 5c.

By these rules, we obtain a cell decomposition C_4 of Q which has no interior vertices. This decomposition contains two congruent triangles and a number of digons. Each digon is mapped to the sphere with a cut along a segment. We break it into two digons by the F-preimage of the complement of this segment in the line that contains it. These lines are shown as red/dotted lines in Fig. 5b,c. After these cuts are made, the number of digons in every "bunch" becomes even. Adding half of them to the adjacent side of the triangle we obtain a decomposition of our torus into two triangles.

The final decomposition of Q into two primitive triangles and digons isometric to half-planes is shown in red/dashed and bold black lines in Figs. 5b,c in two cases: 4b) when C_2 has a diagonal face, and 4c) when it does not.

Now we show that these two triangles are balanced. We refer to the decomposition of a singular triangle described in Proposition 3.2.

Gluing any numbers of half-planes to the sides of a balanced triangle results in a balanced triangle. Primitive triangles are balanced in the following cases. Primitive triangle of the type A is balanced if all angles are less than $\pi/2$. If the greater angle is $> \pi/2$ and at least one half-plane is glued to the opposite side, the resulting triangle is balanced. If the cell decomposition C_2 contains a diagonal face, this implies that at least one half-plane was glued opposite the largest angle of the triangular face. If the triangular face is of the type A, then its longest side is the diagonal, so the largest angle is opposite to it. If this triangle is of type B, then it is balanced (a triangle of this type is always balanced).

If there was no diagonal in C_2, then we obtained triangular faces of C_4 by drawing either the smaller diagonal in a parallelogram, or the exterior diagonal in its exterior which has endpoints at the bigger exterior angles. In both cases the triangle is balanced.

So we obtained a partition of Q into two balanced triangles. We can re-assemble it by moving digons adjacent to a side of Q to the opposite side to make the two balanced triangles congruent. This completes the proof in the non-degenerate case.

Now we consider the degenerate case. $F : Q \to \overline{\mathbf{C}}$ maps the sides of Q into a line ℓ, and we assume without loss of generality that $\ell = \mathbf{R} \cup \{\infty\}$. The images of sides occupy some segment $(a, b) \in \mathbf{R}$, where $a < b$. It is

evident that a and b are the images of two opposite corners of Q. Without loss of generality, these corners are a_1 and a_3. The preimage $F^{-1}(\mathbf{R})$ defines a cell decomposition C_5 of Q. It is exactly of the same type as nets studied in [13]: they consist of simple curves with endpoints at the corners and disjoint interiors, and each curve is mapped homeomorphically onto its image.

Lemma 5.3. *Under these assumptions C_5 contains a curve from a_1 to a_3. So the faces of C_5 are two triangles and several (possibly none) digons.*

Proof. Any component of $F^{-1}((\mathbf{R}\backslash[a,b]) \cup \{\infty\})$ must be a curve from a_1 to a_3 in the interior of Q. This proves the lemma.

Each digon of C_5 is mapped by F to $\overline{\mathbf{C}}$ with a cut (bounded or containing ∞). We partition digons into two halves by complements of these cuts to the $\mathbf{R} \cup \{\infty\}$. Then we split these half-planes in each "bunch" into two equal parts and add them to the corresponding sides of triangular faces. This defines a decomposition of our torus into two triangles. That these triangles are balanced is proved in the same way as in the non-degenerate case. □

This completes the proof of surjectivity of Φ^*. □

6 The spaces $\mathbf{A}_m$, $\mathbf{T}_m$ and $\mathbf{T}_m^*$

6.1 Connected components

To visualize Proposition 3.1, we introduce the *space of angles* $\mathbf{A}_m$. In the intersection of the plane

$$\alpha_1 + \alpha_2 + \alpha_3 = 2m + 1,$$

with the open first octant in $\mathbf{R}^3$ (Fig. 9) we consider the triangle Δ_m defined by the inequalities

$$0 < \alpha_j \le \alpha_i + \alpha_k \quad \text{for all permutations} \quad (i,j,k);$$

it is shaded in Fig. 9. The vertices of Δ_m are

$$(m+1/2, m+1/2, 0), \quad (m+1/2, 0, m+1/2), \quad (0, m+1/2, m+1/2).$$

Notice that the vertices do not belong to Δ_m but the sides do belong, so Δ_m is neither open nor closed.

To obtain $\mathbf{A}_m$ we remove from Δ_m all lines where some α_j is an integer, and add all points where all three α_j are integers. The intersections of lines $\alpha_j = k$ with Δ_m will be called *segments*. A segment is called even or odd depending on the parity of k. There are three families of segments, each containing m segments. Spaces of angles for $m = 1, \dots, 5$ are shown in Figs. 6, 7.

The set $\mathbf{A}_m$ has a natural partition into open topological disks (faces) open intervals (edges) and points (vertices): the faces are components of the interior of $\mathbf{A}_m$ (they are triangles or quadrilaterals), the vertices are the points where all α_j are integers, and the edges are open intervals in $\mathbf{A}_m \cap \partial\Delta_m$. The set of vertices of $\mathbf{A}_m$ will be denoted by $\mathbf{V}_m$.

We have a natural projection

$$\varphi : \mathbf{T}_m \to \mathbf{A}_m \tag{34}$$

which to every balanced triangle puts into correspondence its angles. It follows from Proposition 3.1 that this correspondence is bijective on the part of $\mathbf{T}_m$ where the angles are not integers. This part is mapped bijectively to $\mathbf{A}_m \backslash \mathbf{V}_m$. Triangles with integer angles are mapped to the points of $\mathbf{A}_m$ where all three α_j are integers, and for each integer point in $\mathbf{A}_m$ there are three intervals of $\mathbf{T}_m$ which are mapped to this point.

This induces a partition of $\mathbf{T}_m$: the faces of $\mathbf{T}_m$ are φ-preimages of the faces of $\mathbf{A}_m$, the edges are of two types: interior edges which are mapped by φ to the vertices of $\mathbf{A}_m$ and boundary edges which are mapped bijectively onto intervals of $\mathbf{A}_m \cap \partial\Delta_m$. There are no vertices in this partition of $\mathbf{T}_m$.

The faces of $\mathbf{T}_m$ are adjacent when their images in $\mathbf{A}_m$ share a boundary vertex and *their angles at this vertex are vertical*[5]. Notice that the map ϕ switches the orientation when one passes through any interior edge of $\mathbf{T}_m$ from a face to an adjacent face. This can be seen from the explicit formula for the angles in terms of the conformal coordinate $z = \phi_{i,j,k}$ introduced in Section 4: in the chart where $f(a_1) = 0,\ f(a_2) = 1,\ f(a_3) = z = x + iy$ we have

$$\alpha_1 = p + \arctan(y/x), \quad \alpha_2 = q + \arctan(y/(1-x)),$$

where p, q are integers. Assuming that $x \in (0, 1)$ we compute the Jacobian and see that it is equal to a positive quantity times y, so it switches the sign when y passes through 0.

[5]Opposite angles among the four angles made by crossing of two lines.

Remark. Gluing of two 2-cells along their common boundary 1-cell corresponding to a vertex of $\mathbf{A}_m$ reverses the natural orientation of these 2-cells induced from the (α_1, α_2)-plane. Nevertheless, it is easy to check that the surface $\mathbf{T}_m$ is orientable. To do this one paints the 2-cells of $\mathbf{T}_m$ into two colors, so that each two 2-cells with a common vertex have different colors. See Fig. 8.

To study the surface $\mathbf{T}_m$ we introduce the graph Γ_m, which will be called the *nerve*. Examples of these graphs are shown in figures 5, 6. Their vertices correspond to 2-cells of $\mathbf{T}_m$ (or faces of $\mathbf{A}_m$) and two vertices of Γ_m are connected by an edge if the corresponding two 2-cells of $\mathbf{T}_m$ share an edge or, which is the same, if the corresponding 2-cells of $\mathbf{A}_m$ share a vertex and their angles at this vertex are vertical. Then we find

Proposition 6.1. *When $m \geq 2$, the graph Γ_m has 4 connected components. Exactly one of them, Γ'_m is invariant under the order 3 rotation about the center of $\mathbf{A}_m$. Three others are permuted by this rotation. Γ_1 has only three components, permuted by the rotation. Γ_0 consists of one vertex only.* □

In Fig. 6, Γ'_m is blue/dotted, while in Fig. 7 one of the three components permuted by the order 3 rotation is red, any of these three components is called Γ''_m (they are isomorphic graphs embedded in the plane).

We give first a geometric sketch which makes our proposition evident, and then a more formal proof.

Sketch of a proof of Proposition 6.1. Let us consider the plane

$$P = \{\alpha \in \mathbf{R}^3 : \alpha_1 + \alpha_2 + \alpha_3 = 2m + 1\}.$$

Intersections of P with the planes $\{\alpha_j = \text{integer}\}$ break P into triangles. Connecting the centers of pairs of triangles which share a vertex and whose angles at this vertex are vertical, we obtain four honeycomb structures X_j with disjoint vertices. See Fig. 8 which shows two of these honeycombs. Choosing one vertex of one honeycomb as a center, we see that this honeycomb is invariant under rotation by 120^o about this vertex, while the other three are permuted.

Proof of Proposition 6.1.

Let Δ'_m be the intersection of the plane

$$\alpha_1 + \alpha_2 + \alpha_3 = 2m + 1$$

with the closed first octant $\alpha_j \geq 0,\ 1 \leq j \leq 3$. The *segments*

$$\{(\alpha_1, \alpha_2, \alpha_3) \in \Delta'_m : \alpha_j = k\}, \quad 1 \leq j \leq 3, \quad 0 \leq k \leq 2m$$

divide Δ'_m into open triangles which we call *faces* of Δ'_m. There are three families of these segments, depending on the value of j. A segment with even/odd k will be called an *even/odd*. Since $\alpha_1 + \alpha_2 + \alpha_3$ is odd, among three segments intersecting at an integer vertex, either one or all of them are odd. This implies that a face has either one or three sides on even segments.

We classify faces of Δ'_m into four types:

type I, if all three sides of the triangular face belong to even segments,

type $II_j,\ j \in \{1, 2, 3\}$ if one side belongs to an even segment of family j, while two other sides belong to odd segments of the other two families.

Two faces sharing an integer vertex are called *vertical* if their angles at this vertex are vertical (opposite).

We claim that vertical faces are of the same type. Indeed if the two segments bounding the vertical angles are both even, then each of our two faces must have all three sides on even segments, thus both faces are of type I. If exactly one of the segments is even, and belongs to family j, then both faces are of the type II_j. If both segments are odd, then the sides of our faces opposite to the considered vertex are even and parallel, so they are in the same family and our two faces are in the same family. This proves the claim.

Now we claim that faces of the same type cannot have a common side. If two faces have a common side on an even segment then one of them is of type I and another is of type II. If the common side is on an odd segment then both faces are of type II and their sides on even segments are not parallel. Thus they belong to different types. This proves the claim.

Our next claim is that the closure of the union of faces of the same type is connected. Consider faces of type I. The closure of their union consists of the faces themselves and all even segments. It is clear that the union of all even segments is connected.

The proof for other types is similar: the closure of the union of faces of type II_j consists of the faces themselves, the even segments of family j, and odd segments of two other families. The union of these segments is connected.

If we restrict now to $\mathbf{A}_m$ and consider the union of those faces of a single type which intersect $\mathbf{A}_m$ and their vertices, this union is still connected. Indeed if two faces of one family share a vertex and both intersect $\mathbf{A}_m$ then this common vertex belongs to $\mathbf{A}_m$.

This proves Proposition 6.1. □

Now consider the map $\varphi : \mathbf{T}_m \to \mathbf{A}_m$. Component $\mathbf{L}_m^I$ of $\mathbf{T}_m$ consists of preimages of faces of type I of $\mathbf{A}_m$ and common edges of pairs of these preimages that project to the vertices of faces of type I of $\mathbf{A}_m$. Similarly for $i \in \{1, 2, 3\}$, components II_i of $\mathbf{T}_m$, consist of preimages of faces of type II_i and common edges of pairs of these preimages which project to the vertices of faces of type II_i of $\mathbf{A}_m$. So we obtain

Corollary 6.1. *When $m \geq 2$, $\mathbf{T}_m$ consists of four connected components I, II_1, II_2, II_3. Cyclic permutation of vertices preserves component I and permutes components II_i. As a consequence, $\mathbf{T}_m^*$ has two components, I and II. These components are distinguished by the number of sides with poles:*

When m is even, $\mathbf{L}_m^I$ consists of BFT with no poles on the sides, and $\mathbf{L}_m^{II}$ consists of BFT with two poles on the sides.

When m is odd, $\mathbf{L}_m^I$ consists of BFT with 3 poles on the sides, and $\mathbf{L}_m^{II}$ consists of BFT with one pole on the side. □

Example. Figure 2 shows all types of BFT for $m = 2$ (angle sum 5π). Triangles of types a), b), c) belong to $\mathbf{L}_m^I$. Suppose for example that triangle a) is deformed so that the top vertex moves towards the opposite (horizontal) side. Eventually we obtain a triangle b) with the angles $2\pi, 2\pi, \pi$. If the middle vertex of b) continues moving downwards, we obtain triangle c). Its developing map is 2-to-1 onto the darkly shaded region and 1-to-1 onto the lightly shaded region. There are three types of such triangles c) if the vertices are labeled, but only one type with unlabeled vertices.

Triangles of types d), e), f) belong to $\mathbf{L}_m^{II}$. It is easy to visualize how they are deformed to each other.

Triangles a), b), c) have one pole inside, while triangles d), e), f) have 2 poles, one on each of the two unbounded sides, and the third side is free of poles. Fig. 2 should be compared with Figs. 6, 7, $m = 2$: the set $\mathbf{A}_2$ shows the location of all these triangles in the parameter space.

6.2 Proof of injectivity of Φ^*

We established in Section 4 that $\Phi^*_m : \mathbf{T}^*_m \to \mathbf{L}_m$ is a proper analytic map between punctured surfaces. So to prove injectivity it is sufficient to show that every component of $\mathbf{T}^*_m$ contains an interval I such that for every $T \in I$, T is the unique Φ^*-preimage of $\Phi^*(T)$.

Assume that $m \geq 1$. Then every component contains a triangle with integer angles. Let T be a triangle with integer angles. According to Proposition 3.3 the monodromy group of $\Phi^*(T)$ is a subgroup of a line, so for the torus $\Phi^*(T)$ alternative b) (degenerate case) holds in the proof of surjectivity. It follows that any Φ^*-preimage of $\Phi^*(T)$ also has all integer angles (see Proposition 3.3).

Recall that triangle with integer angles is obtained from a triangle in Fig. 1b in which a_1, a_2, a_3 belong to the same line, by gluing half-planes to the sides (see Proposition 3.2). Let us normalize so that $a_3 = 0$, $a_1 = 1$, and we choose our interval I so that $a_2 := a \in (0, 1/2)$. Then the following properties of $\Phi^*(T)$ are evident:

The shortest non-trivial loop γ_1 based at the singularity has length a_2. We define the orientation of this loop by orienting $(0, a)$ from a to 0 on the boundary of the reduced triangle T'. We recall that the reduced triangle T' is the upper half-plane with corners at $0, a, 1$.

So parameter a is uniquely defined by $\Phi^*(T)$, as the shortest length of a loop based at O on $\Phi^*(T)$. Now we define γ_2 as the loop corresponding to $(a, 1)$ in $\partial T'$, oriented from a to 1. This loop γ_2 is characterized as the shortest loop whose class does not belong to $\mathbf{Z}\gamma_1$.

Each side of T' defines a homotopy class of loops based at O. Two of them are γ_1 and γ_2. Suppose that m_1 half-planes were glued to the side $(0, a)$, and m_2 half-planes were glued to the side $(a, 1)$. Then the torus $\Phi^*(T)$ contains $m_1 + 1$ disjoint (except the base point) geodesic loops in the class $[\gamma_1]$, and $m_2 + 1$ disjoint geodesic loops in the class $[\gamma_2]$.

This implies that the angles $\pi\alpha_i$ of T are defined by the properties of the torus $\Phi^*(T)$, namely $\alpha_i = 1 + m_j + m_k$. This proves injectivity of the map Φ^* and completes the proof of Theorem 1.4.

7 Euler characteristics of components of $\mathbf{L}_m$ and completion of the proof of Theorem 1.1

Theorem 1.4 reduces the study of topology of $\mathbf{L}_m$ to the study of topology of $\mathbf{T}^*_m$.

It is convenient to use the nerves Γ'_m and Γ''_m introduced in Section 6.

First we recall that $\Gamma_m/\mathbf{Z}_3$ consists of 2 components. One of them comes from the component Γ'_m which is invariant with respect to the $\mathbf{Z}_3$ action. This is our component $\mathbf{L}^I_m$. Component $\mathbf{L}^{II}_m$ comes from the three components of Γ''_m which are permuted by the $\mathbf{Z}_3$ action. See Figs. 6, 7.

Computation of the Euler characteristic for component $\mathbf{L}^I_m$.

Let Γ'_m be the component of Γ_m which is invariant with respect to the $\mathbf{Z}_3$ action. The numbers ϵ_0, ϵ_1 are defined in the statement of Theorem 1.1. We add to them ϵ_2 and interpret these numbers in terms of $\mathbf{A}_m$:

$\epsilon_0 = 1$ if the center of $\mathbf{A}_m$ belongs to a 2-cell. Equivalent condition is that a vertex of Γ'_m is fixed by the $\mathbf{Z}_3$ action.

$\epsilon_1 = 1$ if there is a vertex of Γ'_m representing a face which has the middle of the side of Δ_m on the boundary.

$\epsilon_2 = 1$ if there is a vertex of Γ'_m representing a face which has a corner of Δ_m on the boundary.

We introduce further notation:

V_1, V_2, V_3 are the numbers of vertices of Γ'_m of degrees $1, 2, 3$, and V is the total number of vertices.

E is the number of edges of Γ'_m.

Taking into account all identifications on Γ'_m, we obtain the following formula for the Euler characteristic:

$$\chi(\mathbf{L}^I_m) = E/3 - V_1/6 - V_2/2 - 2V_3/3 + 2\epsilon_0/3 + (\epsilon_1 - \epsilon_2)/2. \qquad (35)$$

It is easy to see that for odd m

$$E = 3(m^2-1)/8, \quad V_1 = 3(m-1)/2, \quad V_2 = 0, \quad V = (m^2+4m-5)/4,$$

and V_3 can be computed by the formula $V_3 = V - V_1 - V_2$. This gives the formula for $\chi(\mathbf{L}^I_m)$ when m is odd. When m is even, we have

$$E = 3(m^2+2m)/8, \quad V_1 = 3, \quad V_2 = 3(m-1)/2, \quad V = (m/2+1)^2,$$

and again $V_3 = V - V_1 - V_2$. This gives the formula for $\chi(\mathbf{L}_m^I)$ when m is even.

Computation of the Euler characteristic of component $\mathbf{L}_m^{II}$

Let Γ_m'' be one of the three components of Γ_m which are permuted by the $\mathbf{Z}_3$ action. We use the following notation

E is the number of edges of Γ_m''

V_1, V_2, V_3 and V are the numbers of vertices of Γ_m'' of orders $1, 2, 3$ and the total number of vertices.

ϵ_1 and ϵ_2 have the same meaning as before.

For the Euler characteristic we have in this case

$$\chi(\mathbf{L}_m^{II}) = E + (3/2)V_1 + V_2/2 - 2V + (\epsilon_1 - \epsilon_2)/2.$$

When m is odd,

$$E = (3m^2{+}4m{+}1)/8, \quad V_1 = (m{+}3)/2, \quad V_2 = m{-}1, \quad V = (m^2{+}4m{+}3)/4.$$

When m is even,

$$E = (3m^2 + 2m)/8, \quad V_1 = m, \quad V_2 = m/2, \quad V = (m/2+1)^2 - 1.$$

This gives the formula for $\chi(\mathbf{L}_m^{II})$.

Computation of the number of punctures.

Consider a small simple loop around a puncture of $\mathbf{T}_m^*$. This loop projects to a contour in $\mathbf{A}_m$ which goes close to the lines $\alpha_j = k$, switching the side at each integer point. For component $\mathbf{L}_m^I$, the contour goes near lines with the same even k, and $j = 1, 2, 3$ and closes. See Fig. 10. So there is a $1-1$ correspondence between these contours and triples of segments (one in each family) with even k. So there are $\lfloor m/2 \rfloor$ of such loops. In addition, when m is even there is a puncture corresponding to the vertices of Δ_m. Thus the total number of punctures on $\mathbf{L}_m^I$ is $m/2+1$ when m is even and $(m-1)/2$ when m is odd. In other words, the number of punctures on Component $\mathbf{L}_m^I$ equals

$$h_m^I := d_m^I, \tag{36}$$

where d_m^I was defined in (8).

For component $\mathbf{L}_m^{II}$, the computation is similar, see Fig. 11. Each contour goes either near an even segment, in which case it closes after describing three

segments, one of each family. If a contour accompanies an odd segment, it ends on the other side of the odd segment after describing three segments. So the total number of contours is m when m is even and $m+1$ when m is odd, in other words

$$h_m^{II} := 2\lceil m/2 \rceil = 2d_m^{II}/3. \tag{37}$$

Component $\mathbf{L}_m^I$

m	ϵ_0	ϵ_1	ϵ_2	V_1	V_2	V_3	E	V	χ	h	g	d
2	1	0	1	3	0	1	3	4	0	2	0	2
3	1	1	0	3	0	1	3	4	1	1	0	1
4	0	1	1	3	3	3	9	9	-1	3	0	3
5	1	0	0	6	0	4	9	10	0	2	0	2
6	1	0	1	3	6	7	18	16	-2	4	0	4
7	0	1	0	9	0	9	18	18	-1	3	0	3
8	1	1	1	3	9	13	30	25	-3	5	0	5
9	1	0	0	12	0	16	30	28	-2	4	0	4
10	0	0	1	3	12	21	45	36	-6	6	1	6
11	1	1	0	15	0	25	45	40	-3	5	0	5
12	1	1	1	3	15	31	63	49	-7	7	1	7
13	0	0	0	18	0	36	63	54	-6	6	1	6

Component $\mathbf{L}_m^{II}$

m	ϵ_1	ϵ_2	V_1	V_2	V_3	E	V	χ	h	g	$d/3$
1	0	0	2	0	0	1	2	0	2	0	1
2	0	1	2	1	0	2	3	0	2	0	1
3	1	0	3	2	1	5	6	-2	4	0	2
4	1	1	4	2	2	7	8	-2	4	0	2
5	0	0	4	4	4	12	12	-4	6	0	3
6	0	1	6	3	6	15	15	-4	6	0	3
7	1	0	5	6	9	22	20	-8	8	1	4
8	1	1	8	4	12	26	24	-8	8	1	4
9	0	0	6	8	16	35	30	-12	10	2	5
10	0	1	10	5	20	40	35	-12	10	2	5
11	1	0	7	10	25	51	42	-18	12	4	6
12	1	1	12	6	30	57	48	-18	12	4	6

We include two tables for $1 \leq m \leq 13$. Notation, besides that already introduced is: g for the genus, h for the number of punctures, d for the degree of the forgetful map as in (8), (9). The formulas for the degrees follow from [30, sections 23.21-23.24].

Remark. There is an alternative method of counting the punctures, based on the description on compactifications of the spaces of Abelian differentials in [3].

Orbifold points.

By definition, an orbifold point in $\mathbf{L}_m$ is a point which corresponds to a flat singular torus with a non-trivial automorphism. An automorphism here means an orientation-preserving isometry. The trivial automorphism is the involution which exists on every flat singular torus. There are two types of tori with non-trivial automorphisms: hexagonal ones with an automorphism of order 3, and square ones, with non-trivial automorphism of order 4. In the representation of tori as $\Phi^*(T)$, hexagonal tori correspond to triangles whose all angles are equal, while square tori correspond to marginal triangles whose two smaller angles are equal. So in the space of angles $\mathbf{A}_m$, the hexagonal torus arises from the center of Δ_m when this center belongs to $\mathbf{A}_m$, and the square torus corresponds to the middles of the sides of Δ_m. In Figs. 6, 7, these points are denoted by little circles in the center of the picture, and little black triangles in the middles of the sides.

In the next section we will use the following

Proposition 7.1. *In the Lamé equation (2) or (3) corresponding to a hexagonal or square torus (in the metric sense), the accessory parameter λ is equal to* 0 *(see the text after (4)).*

Proof. Since a metric automorphism is also a conformal automorphism, it corresponds to an automorphism of the Lamé equation, that is to a fixed point of transformation (4). For both fixed points we have $\lambda = 0$. □

8 Theorem 1.2 and Maier's conjecture

To prove Theorem 1.2 and its corollaries we first state the exact relation between $\mathbf{L}_m$ and $\mathbf{H}_m$.

A *marked* elliptic curve is an elliptic curve on which the three points of (exact) order 2 are labeled. Legendre's family (14) parametrizes marked

elliptic curves: the labels are $0, 1, a$. The permutation group S_3 acts on the space of marked elliptic curves by permuting the labels. Explicitly, the orbit of a under this action is

$$a, \quad 1-a, \quad 1/a, \quad 1-1/a, \quad 1/(1-a), \quad a/(a-1). \tag{38}$$

This action lifts to the moduli space $\mathbf{C} \times \mathbf{C}_a$ of Lamé equations in the form of Legendre: the generators $a \mapsto 1-a$ and $a \mapsto 1/a$ lift to

$$(B, a) \mapsto (-B - m(m+1),\ 1-a)\,, \quad \text{and}$$

$$(B, a) \mapsto (B/a,\ 1/a)\,.$$

To obtains these two transformations, one changes the independent variable in (16) to $\zeta = 1 - z$ and $z = z/a$, respectively. Taking the quotient of the space $\mathbf{C}\times\mathbf{C}_a$ of equations (16) by this S_3 action we obtain an orbifold covering Ψ_m of degree 6 from the moduli space of equations (16) to the moduli space Lame_m, such that the following diagram is commutative:

$$\begin{array}{ccc} \mathbf{H}_m^j & \xrightarrow{\Psi_m^j} & \mathbf{L}_m^K \\ \Big\downarrow \sigma_m & & \Big\downarrow \pi_m \\ \mathbf{C}_a & \xrightarrow{\psi} & \mathbf{C}_J \end{array} \tag{39}$$

Here Ψ_m^j are restrictions of Ψ_m on $\mathbf{H}_m^j$, and $K = I$ for $j = 0$, $K = II$ for $j \in \{1, 2, 3\}$. (We have not proved yet that $\mathbf{H}_m^j$ are irreducible; this will be done only in the end of this section).

The explicit expression of ψ is in (15). To obtain an explicit expression of Ψ_m we change the independent variable x in the equation (16) to $z = z - (1+a)/3$. Then we easily obtain $\Psi_m = (R_1, R_2, R_3)$ modulo scaling (4), where

$$\begin{aligned} \lambda &= R_1(B, a) := B + m(m+1)(a+1)/3, \\ g_2 &= R_2(B, a) := 4(a^2 - a + 1)/3, \\ g_3 &= R_3(B, a) := 8(a^3 - 3a^2/2 - 3a/2 + 1)/27. \end{aligned} \tag{40}$$

We define compact Riemann surfaces $\overline{\mathbf{L}}_m^K$, $\overline{\mathbf{H}}_m^j$, $\overline{\mathbf{C}}_J$ and $\overline{\mathbf{C}}_a$ by filling the punctures. Later we will endow them with orbifold structures. The forgetful maps π_m, σ_m and maps $\psi,\ \Psi$ extend uniquely to these compactifications.

Definition 8.1. *A point $x \in \overline{\mathbf{L}}_m$ is called special if $\pi_m(x) \in \{0, 1, \infty\}$. A point $x \in \overline{\mathbf{H}}_m$ is called special if*

$$\sigma_m(x) \in \{0, 1, \infty, 2, 1/2, -1, (1 \pm i\sqrt{3})/2\}.$$

Since $\Psi_m^j : \mathbf{H}_m^j \to \mathbf{L}_m^j$ are orbifold coverings, the maps $\Psi_m^j : \overline{\mathbf{H}}_m^j \to \overline{\mathbf{L}}_m^K$ can be ramified only at special points.

Next we study ramification properties of forgetful maps at the special points. For this we need two lemmas, the first one is classical, see for example [15, Ch. II, §1, Thm 1]:

Lemma 8.1. *Let $A = (a_{i,j})$ be an $n \times n$ matrix with $a_{i,i+1} > 0,\ 1 \le i \le n-1$, and $a_{i,i-1} > 0,\ 2 \le i \le n$, the rest of the entries are zeros. Then all roots of the characteristic polynomial are real and simple. The characteristic polynomial is either even or odd, in other words it has the form $\lambda^k P(\lambda^2)$, where $k \in \{0, 1\}$.* □

The second lemma was communicated to us by V. Tarasov; it is inspired by [28, Prop. 3]:

Lemma 8.2. *Let $A = (a_{i,j})$ be an $n \times n$ matrix with $a_{i,i+1} > 0,\ 1 \le i \le n-1$ and $a_{i,i-2} > 0,\ 3 \le i \le n$, the rest of the entries are zeros. Then all roots of the characteristic polynomial, except possibly 0, are simple and their arguments are of the form $2\pi k/3,\ k \in \{0, 1, 2\}$. In fact this characteristic polynomial has the form $\lambda^k P(\lambda^3)$, where $k \in \{0, 1, 2\}$ and P is a real polynomial with all roots positive.*

A proof of Lemma 8.2 will be given in the next section.

The following proposition lists ramification of forgetful maps over special points.

Proposition 8.1. 1. *Ramification of π_m^K over special points is the following:*
Over $J = 0$ there are $\lfloor d_m^K/3 \rfloor$ triple points, and one additional point x when d is not divisible by 3. This additional point x is the orbifold point of order 3, and π_m^K has x as a double point when $d \equiv 2 \pmod 3$, and a simple point when $d \equiv 1 \pmod 3$.
Over $J = 1$ there are $\lfloor d_m^K/2 \rfloor$ double points, and one simple point when d_m^K is odd. This simple point is the orbifold point of order 2.
Over $J = \infty$ there are $d_m^{II}/3$ double points when $K = II$. The rest $d_m^{II}/3$ points are simple. For $K = I$ all points over ∞ are simple.

2. *Ramification of σ_m^j over special points is the following: Over each $a = 1/2 \pm i\sqrt{3}/2$, there is one double point when $d_m^j \equiv 2 \pmod 3$. There is no other ramification over special points.*

Proof. For component $\mathbf{L}_m^I$ with even m and $J = 0$, we consider polynomial solutions Q of equation (2) with $g_2 = 0,\ g_3 = 1$, that is

$$(4x^3 - 1)Q'' + 6x^2Q' - (m(m+1)x + \lambda)\, Q = 0.$$

The matrix of the linear operator in the left-hand side in the basis of monomials has the form as in Lemma 8.2. Therefore the characteristic polynomial of this matrix has the form $\lambda^k P(\lambda^3)$. This has a root of multiplicity 2 at 0 when $d \equiv 2 \pmod 2$. Other roots come in triples, each triple lies on the same orbit under the C^* action (4), so we have $\lfloor d_m^K/3 \rfloor$ triple points.

Similar considerations apply to other special points.

For component $\mathbf{L}_m^I$ with odd m and $J = 0$, we consider solutions of (2) of the form $\sqrt{4x^3 - g_2x - g_3}\, Q(x)$, where Q is a polynomial. The equation for Q becomes

$$(4x^3 - 1)Q'' + 18x^2Q' + ((12 - m(m+1))\, x - \lambda)\, Q = 0,$$

and this leads to a matrix of the same form described in Lemma 8.2, so the same argument as in the case of even m applies.

For component $\mathbf{L}_m^I$ with even m and $J = 1$, we set $g_2 = 1, g_3 = 0$, and obtain

$$(4x^3 - x)Q'' + (6x^2 - 1/2)Q' - (m(m+1)x + \lambda)\, Q = 0$$

which leads to a matrix described in Lemma 8.1. The characteristic polynomial is of the form $\lambda^k P(\lambda^2),\ k \in \{0, 1\}$ which has one simple root $\lambda = 0$ when $k = 1$ and other roots come in pairs which are on the same orbit under the $\mathbf{C}^*$ action.

For component $\mathbf{L}_m^I$ with odd m and $J = 1$ we obtain the equation

$$(4x^3 - x)Q'' + (18x^2 - 3/2)Q' + ((12 - m(m+1))\, x - \lambda)\, Q = 0$$

which again leads to a matrix described in Lemma 8.1. The conclusion is similar.

For component $\mathbf{L}_m^{II}$ we use the Legendre's form of Lamé equation (16). When m is odd, and $j = 1$, we plug the solution of the form $\sqrt{z}\,Q(z)$ and obtain

$$\begin{aligned} & 4z(z-1)(z-a)Q'' + (10z^2 + 8z(1+a) + 6a)Q' \\ - \quad & \big((m^2 - m - 2)z + 1 + a + B\big)\,Q = 0. \end{aligned}$$

When m is even, and $j = 1$, we plug the solution of the form $\sqrt{z(z-1)}\,Q(z)$ and obtain

$$\begin{aligned} & 4z(z-1)(z-a)Q'' + (14z^2 - (12a+8)z + 6a)Q' \\ - \quad & \big((m^2 + m - 6)z + B + 4a + 1\big)\,Q = 0. \end{aligned}$$

Both these equations lead to Jacobi matrices as in Lemma 8.1.

To study ramification at the punctures, we use again Legendre's form. Take, for example, $a = 0$. The matrix of the operator in the left-hand side of (3) is triangular, with distinct eigenvalues. So σ_m is unramified at a point x with $\sigma_m(x) = 0$. Now we have $\deg_0 \psi = 2$, so by (39)

$$\deg_{\Psi_m(x)}(\pi_m) \cdot \deg_x \Psi_m = 2,$$

thus each multiple is either 1 or 2. But we know the total number of points in $\mathbf{L}_m^K$ over $J = \infty$ (punctures) and this implies the statement of Proposition 8.1 for $J = \infty$.

That π_m is an orbifold map follows from the identification of the orbifold points in $\mathbf{L}_m^K$ in Proposition 7.1. □

The difference between π_m and σ_m is that there is no $\mathbf{C}^*$ action in the second case.

Proposition 8.1 together with relation (39) and known ramification of ψ allows us to define the orbifold structure on the compactified spaces, so that ψ and Ψ_m become orbifold coverings.

For what follows we define compactifications of our orbifolds:

$$\overline{\mathbf{C}}_J = \overline{\mathbf{C}}(0(3), 1(2), \infty(2)), \quad \overline{\mathbf{C}}_a = \overline{\mathbf{C}}.$$

Then $a \mapsto J = \psi(a)$ which is defined in (15) is an orbifold covering. Then we define $\overline{\mathbf{L}}_m^K$ by adding the punctures x, $\pi_m^K(x) = \infty$, and defining $n(x) = 1$ if $\deg_x(\pi_m^K) = 2$ and $n(x) = 2$ when $\deg_x(\pi_m^K) = 1$. Finally we define $\overline{\mathbf{C}}_a$ as

the Riemann sphere with $n(a) = 1$ for all a, and define $\overline{\mathbf{H}}^j_m$ as $\mathbf{H}^j_m$ with filled punctures. The orbifold structure on $\overline{\mathbf{H}}^j_m$ is trivial: $n(x) \equiv 1$. With these definitions Theorem 1.1 gives:

$$\chi^O(\overline{\mathbf{L}}^K_m) = \chi^O(\mathbf{L}^K_m) + d^K_m/2. \tag{41}$$

Proposition 8.2. *The following diagram is commutative:*

$$\begin{array}{ccc} \overline{\mathbf{H}}^j_m & \xrightarrow{\Psi^j_m} & \overline{\mathbf{L}}^K_m \\ \big\downarrow \sigma_m & & \big\downarrow \pi_m \\ \overline{\mathbf{C}}_a & \xrightarrow{\psi} & \overline{\mathbf{C}}_J \end{array} \tag{42}$$

Here all four spaces are orbifolds, with orbifold functions just defined, the horizontal arrows are orbifold coverings, and vertical arrows are maps of orbifolds. We have

$$\deg \Psi^0_m = 6 \quad \textit{and} \quad \deg \Psi^j_m = 2, \quad j \in \{1, 2, 3\}.$$

Furthermore,

$$\chi(\overline{\mathbf{H}}^0_m) = \chi^O(\overline{\mathbf{H}}^0_m) = 6\chi^O(\overline{L}^I_m), \tag{43}$$

$$\chi(\overline{\mathbf{H}^j_m}) = \chi^O(\overline{\mathbf{H}}^j_m) = 2\chi^O(\overline{L}^{II}_m). \tag{44}$$

Proof. Since in the diagram (39) the horizontal arrows are orbifold coverings and vertical arrows are orbifold maps, it remains to check the points over $J = \infty$ and over $a \in \{0, 1, \infty\}$. That $\psi : \overline{\mathbf{C}}_a \to \overline{\mathbf{C}}_J$ is an orbifold covering is well known and follows from the explicit formula (15).

Let $x \in \mathbf{H}^j_m$, $\sigma_m(x) \in \{0, 1, \infty\}$. By Proposition 8.1, $\deg_x(\sigma_m) = 1$ and we know that $\deg_{\sigma(x)}(\psi) = 2$. Therefore,

$$\deg_x(\Psi^j_m) \cdot \deg_{\Psi^j_m(x)}(\pi_m) = 2,$$

thus $\deg_x \Psi^j_m$ is either 1 or 2, and the definition of $n(\Psi^j_m(x))$ ensures that Ψ^j_m is an orbifold covering.

That the vertical arrows are orbifold maps follows from Proposition 8.1. Formulas (43), (44) follow from (7). □

Now we are ready to prove Theorem 1.2.

Proposition 8.3. *The curves $\overline{\mathbf{H}}^j_m$ are irreducible and non-singular.*

Proof. Using (7), (41) and (43), we obtain

$$\begin{aligned} 2-\chi(\overline{\mathbf{H}}^0_m) &= 2-6\chi^O(\overline{\mathbf{L}}^I_m) = 2-6\chi^O(\mathbf{L}^I_m) - 3d \\ &= 2+(d^I_m)^2 - 3d^I_m = (d^I_m-1)(d^{II}_m-2). \end{aligned}$$

Similarly, using (7), (41) and (44), we obtain

$$\begin{aligned} 2-\chi(\overline{\mathbf{H}}^j_m) &= 2-2\chi^O(\overline{\mathbf{L}}^j_m) = 2-2\chi^O(\mathbf{L}^j_m) - d^{II}_m \\ &= 2+(d^{II}_m)^2/9 - d^{II}_m = (d^{II}_m/3-1)(d^{II}_m/3-2), \quad j\in\{1,2,3\}. \end{aligned}$$

Therefore, in any case we have

$$2-\chi(\overline{\mathbf{H}}^j_m) = (\deg\overline{\mathbf{H}}^j_m - 1)(\deg\overline{\mathbf{H}}^j_m - 2). \tag{45}$$

Suppose that for some j and m, $\overline{\mathbf{H}}^j_m$ has N irreducible components of degrees d_k genera g_k and degrees d_k for $1\le k\le N$. Then

$$\deg\overline{\mathbf{H}}^j_m = \sum_{k=1}^N d_k, \quad \chi(\overline{\mathbf{H}}^j_m) = \sum_{k=1}^N \chi_k, \tag{46}$$

$$\chi_k = 2-2g_k, \quad \text{and} \quad 2g_k \le (d_k-1)(d_k-2); \tag{47}$$

the last inequality follows from (18). Substituting the expressions $\deg\overline{\mathbf{H}}^j_m$ and $\chi(\overline{\mathbf{H}}^j_m)$ from (46) to (45) and using (47) we obtain after simple manipulation

$$\left(\sum_{k=1}^N d_k\right)^2 \le \sum_{k=1}^N d_k^2;$$

since all $d_k\ge 1$, this is possible only when $N=1$. Thus $\overline{\mathbf{H}}^j_m$ is irreducible. Then from (45) we obtain its genus,

$$g(\overline{\mathbf{H}}^k_m) = (2-\chi(\overline{\mathbf{H}}^j_m)/2 = (\deg\overline{\mathbf{H}}^j_m - 1)(\deg\overline{\mathbf{H}}^j_m - 2)/2,$$

so it is non-singular since it satisfies (18) with equality. □

This proposition completes the proof of Theorem 1.2.

Proof of Corollary 1.1.

Consider the map $R : \mathbf{H}_m \to \{F_m(\lambda, g_2, g_3) = 0\}$ defined in (40). We will show that it is transversal to the orbits of the $\mathbf{C}^*$ action (4) at non-special points.

A trajectory of restriction of this action onto the (g_2, g_3) plane has the form $(g_2, g_3) = (t^2, ct^3)$, $t \in \mathbf{C}^*$, so the tangent vector is $(2t, 3ct^2)$ which is parallel to $(2/g_3, 3/g_2) = (2/R_3, 3/R_2)$. If the vectors $(2/R_3, 3/R_2)$ and (R_2', R_3') are collinear, we must have

$$S := R_2 R_3 (3R_2'/R_2 - 2R_3'/R_3) = 0.$$

But an explicit computation shows that

$$S = -16a(a-1)/3,$$

which can be zero only at the special points.

Therefore the maps Ψ_m^j are ramified only at the special points. Diagram (42) is clear from the definition. □

Proof of Corollary 1.2.

We compute the ramification of the forgetful map π and then make the correction for special points.

The usual (not orbifold) Euler characteristic of the compactification of $\mathbf{L}_m^I$ is $\chi(\overline{\mathbf{L}}_m^I) = \chi(\mathbf{L}_m^I) + h$, where h equals the number of punctures. So from Theorem 1.1 for $\mathbf{L}_m^I$ and Riemann–Hurwitz formula the total ramification of π is

$$\begin{aligned} & 2d - \chi(\overline{\mathbf{L}}_m^I) = 2d - \chi(\mathbf{L}_m^I) - h = d - \chi(\mathbf{L}_m^I) \\ = \;& d + d^2/6 - (4\epsilon_0 + 3\epsilon_1)/6 \\ = \;& \lfloor (d^2 - d + 4)/6 \rfloor + 2\lfloor d/3 \rfloor + \lfloor d/2 \rfloor, \end{aligned}$$

where $d = \deg_\lambda F_m^I$. The first summand is the degree of the Cohn polynomial, and the other two reflect the additional ramification over the special points 0 and 1 (Proposition 8.1). Indeed, since the only singularities of the surface $F_m^I(\lambda, g_2, g_3) = 0$ lie over $g_2 = 0$ and $g_3 = 0$, zeros of the Cohn polynomial at all points $J \in \mathbf{C} \backslash \{0, 1\}$ come from ramification points of π. For $J = 0$, our curve has the form $\lambda_k P(\lambda^3)$, where P has only simple zeros, so only $\lambda = 0$ is a multiple zero when $k = 2$. Other ramification points of π over $J = 0$ are not zeros of Cohn's polynomial.

Similarly, $J = 1$ is not a zero of Cohn's polynomial.

For $\mathbf{L}_m^{II}$ the total ramification is

$$d + d^2/18 - (1 - \epsilon_1)/2 = (d/3)(d/3 - 1)/2 + 2d/3 + \lfloor d/2 \rfloor.$$

where $d = \deg_\lambda F_m^{II}$. Again, the first summand corresponds to the degree of the Cohn polynomial while the other two reflect additional ramification over the special points (Proposition 8.1). □

Next we briefly describe an alternative approach to our main results. The following remarks are not necessary for understanding the rest of the paper.

Remarks on parametrization of $\mathbf{H}_m$ by a space of triangles

In the beginning of the previous section we mentioned that $\mathbf{H}_m$ represents the space of marked singular tori.

In view of the above interpretation of $\mathbf{H}_m$, we can construct a natural lift of the isomorphism $\Phi^* : \mathbf{T}_m^* \to \mathbf{L}_m$ to an isomorphism $\widehat{\Phi}^* : \widehat{\mathbf{T}}_m^* \to \mathbf{H}_m$ that makes the following diagram commutative:

$$\begin{array}{ccc} \widehat{\mathbf{T}}_m^* & \xrightarrow{\Sigma} & \mathbf{T}_m^* \\ \big\downarrow \widehat{\Phi}^* & & \big\downarrow \Phi^* \\ \mathbf{H}_m & \xrightarrow{\Psi} & \mathbf{L}_m \end{array}$$

Here $\widehat{\mathbf{T}}_m^*$ is a suitable space of flat singular triangles. The point is that one could fully describe the topology of the open Riemann surface $\widehat{\mathbf{T}}_m^*$ and so of $\mathbf{H}_m$ in a direct way, and from that deduce the topology of $\mathbf{L}_m$ by taking the quotient by a natural S_3-action described below.

Recall that in a balanced flat singular triangle $(D, \{a_i\}, f) \in \mathbf{T}_m$, the cyclic order of the corners (a_1, a_2, a_3) on ∂D matches the orientation induced by the developing map f, and that we coordinatize $\mathbf{T}_m$ using the functions $\phi_{i,j,k}$. Denote by $-\mathbf{T}_m$ the space of balanced flat singular triangles $(D, \{a_i\}, f)$ for which the cyclic order (a_1, a_3, a_2) matches the orientation induced by f, and coordinatize $-\mathbf{T}_m$ using the complex conjugates $\bar{\phi}_{i,j,k}$. Moreover, let $\widehat{\mathbf{T}}_m$ be the disjoint union of $\mathbf{T}_m$ and $-\mathbf{T}_m$. The permutation group S_3 acts on $\widehat{\mathbf{T}}_m$ by relabeling the corners.

By identifying each marginal triangle $(D, \{a_i\}, f) \in \widehat{\mathbf{T}}_m$ with its conjugate $(D, \{a_i\}, \bar{f})$, we obtain a space $\widehat{\mathbf{T}}_m^*$. It is immediate that the charts defined

above for $\widehat{\mathbf{T}}_m$ induce a complex structure on $\widehat{\mathbf{T}}^*_m$, and that the S_3-action descends to $\widehat{\mathbf{T}}^*_m$. The quotient space $\widehat{\mathbf{T}}^*_m/S_3$ is naturally identified with $\mathbf{T}^*_m$ and such identification induces the map Σ.

Moreover, to a triangle T in $\widehat{\mathbf{T}}_m$ we can associate the torus $\Phi(T)$ with the marking $t(T) = (t_1, t_2, t_3)$, where t_1, t_2, t_3 are the midpoints of $[a_1, a_2]$, $[a_1, a_3]$, $[a_2, a_3]$ respectively. Thus we can define $\widehat{\Phi}^*(T) = (\Phi(T), t(T))$. Since the diagram is manifestly commutative, the map $\widehat{\Phi}^* : \widehat{\mathbf{T}}_m \to \mathbf{H}_m$ is an isomorphism of Riemann surfaces (with trivial orbifold structure on both surfaces), and Σ is an orbifold cover.

Connected components of $\mathbf{H}_m$ can be studied by analyzing $\widehat{\mathbf{T}}^*_m$, instead of exploring the orbifold cover Ψ_m as we did in the previous section. Similarly to what we did with $\mathbf{T}_m$, we can construct a nerve graph $\widehat{\Gamma}_m$ analogous to Γ_m. It consists of the disjoint union of two isomorphic components: Γ_m associated to $\mathbf{T}_m$ and $-\Gamma_m$ associated to $-\mathbf{T}_m$. Note that, if v is a *lateral vertex* of Γ_m, namely a vertex corresponding to a face of $\mathbf{A}_m$ adjacent to a boundary edge in $\partial\Delta_m$, then the preimage of v and the preimage of $-v$ belong to the same connected component of $\widehat{\mathbf{T}}^*_m$. Since each component of Γ_m has a lateral vertex, it follows that every component of Γ_m exactly corresponds to a component in $\widehat{\mathbf{T}}^*_m$, which thus has four connected components.

Similarly to what was done in Section 7 one can also compute the genera of $\mathbf{H}^j_m$ using the parametrization $\widehat{\Phi} : \widehat{\mathbf{T}}^*_m \to \mathbf{H}_m$ and obtain an alternative proof of our results about $\mathbf{H}_m$ in this section. Once the number of components, their genera and non-singularity are established for $\mathbf{H}_m$, one can obtain Theorem 1.1 via (42).

9 Proof of Lemma 8.2

In this section, we give a proof of Lemma 8.2 which is due to V. Tarasov. It is inspired by an argument from [28, Proposition 3] which was brought to our attention by Eduardo Chavez Heredia from the University of Bristol.

The proof is a generalization of the classical arguments, going back to Ch. Sturm, which are used in the proof of Lemma 8.1.

Let $D = \{d_{i,j}\}$ be an $n \times n$ matrix with entries

$$\begin{aligned} d_{i,i} &= s, \qquad i = 1, \dots, n, \\ d_{i,i+1} &= a_i, \qquad i = 1, \dots, n-1, \\ d_{i,i-2} &= b_i, \qquad i = 3, \dots, n. \end{aligned}$$

and consider the principal minors

$$D_k = \det(d_{ij})_{i,j=1,\dots,k}$$

They satisfy the recurrences

$$D_{k+3} = sD_{k+2} + c_k D_k,$$

where

$$c_k = a_{k+1}a_{k+2}b_{k+3} > 0,$$

with the initial conditions

$$D_0 = 1, \quad D_1 = s, \quad D_2 = s^2.$$

Then

$$D_{3j}(s) = P_j(s^3), \quad M_{3j+1}(s) = sQ_j(s^3), \quad D_{3j+2}(s) = s^2 R_j(s^3)$$

where the polynomials P_j, Q_j, R_j satisfy the recurrences

$$P_{j+1} = sR_j + A_j P_j, \tag{48}$$

$$Q_{j+1} = P_{j+1} + B_j Q_j, \tag{49}$$

$$R_{j+1} = Q_{j+1} + C_j R_j, \tag{50}$$

where

$$A_j = c_{3j}, \quad B_j = c_{3j+1}, \quad C_j = c_{3j+2}$$

and the initial conditions

$$P_0 = Q_0 = R_0 = 1. \tag{51}$$

Lemma 9.2 follows from

Proposition 9.1. *Let us define polynomials $P_j(s), Q_j(s), R_j(s)$ by recurrences (48), (49), (50) where all A_j, B_j, C_j are strictly positive, and initial conditions (51). Then all polynomials P_j, Q_j and R_j, $j = 1, \dots$ are monic, have degree j and positive coefficients, and all their roots are negative and simple. Moreover, if $p_{j1} > \dots > p_{jj}$, $q_{j1} > \dots > q_{jj}$, $r_{j1} > \dots > r_{jj}$, are respective roots of the polynomials P_j, Q_j, R_j, then $p_{jk} > q_{jk} > r_{jk}$ for all $k = 1, \dots, j$, and $r_{jk} > p_{j,k+1}$ for all $k = 1, \dots, j-1$.*

Proof. We prove this by induction. It is evident that our polynomials are monic and have positive coefficients. Therefore their real roots are negative. To find the number of real roots and to show that they are interlacent we look at the signs of our polynomials at the roots of other polynomials using (48)–(50). The base of induction is given by $j = 1$ and is clear. The induction procedure is as follows.

By (48) and the induction assumption,

$$P_{j+1}(0)\, P_{j+1}(p_{j1}) \;=\; p_{j1} A_j P_j(0)\, R_j(p_{j1}) < 0\,,$$

$$P_{j+1}(r_{jk})\, P_{j+1}(p_{j,k+1}) \;=\; p_{j,k+1} A_j P_j(r_{jk})\, R_j(p_{j,k+1}) < 0\,,$$

for all $k = 1, \dots, j-1$, and

$$(-1)^j P_{j+1}(r_{jj}) = (-1)^j A_j P_j(r_{jj}) > 0\,.$$

This implies that P_{j+1} has roots $p_{j+1,k},\ k = 1, \dots, j+1$, located as follows:

$$0 > p_{j+1,1} > p_{j1}\,, \quad r_{j,k-1} > p_{j+1,k} > p_{jk}\,,\ \ k = 2, \dots, j\,, \quad r_{jj} > p_{j+1,j+1}\,. \tag{52}$$

Thus all roots of P_{j+1} are negative and simple.

By the induction assumption and (52),

$$p_{j+1,1} > q_{j1}\,, \quad q_{j,k-1} > p_{j+1,k} > q_{jk}\,,\ \ k = 2, \dots, j\,, \quad q_{jj} > p_{j+1,j+1}\,. \tag{53}$$

Then by (49) and (53),

$$Q_{j+1}(p_{j+1,k})\, Q_{j+1}(q_{jk}) \;=\; B_j Q_j(p_{j+1,k})\, P_{j+1}(q_{jk}) < 0\,,$$

for all $k = 1, \dots, j$, and

$$(-1)^j Q_{j+1}(p_{j+1,j+1}) = (-1)^j B_j Q_j(p_{j+1,j+1}) > 0\,.$$

This implies that Q_{j+1} has roots $q_{j+1,k},\ k = 1, \dots, j+1$, located as follows:

$$p_{j+1,k} > q_{j+1,k} > q_{jk}\,,\ \ k = 1, \dots, j\,, \quad p_{j+1,j+1} > q_{j+1,j+1}\,. \tag{54}$$

Thus all roots of Q_{j+1} are negative and simple.

By the induction assumption, (54), and (52),

$$q_{j+1,1} > r_{j1}\,, \quad r_{j,k-1} > q_{j+1,k} > r_{jk}\,,\ \ k = 2, \dots, j\,, \quad r_{jj} > q_{j+1,j+1}\,. \tag{55}$$

Then by (50) and (55),

$$R_{j+1}(q_{j+1,k})\,R_{j+1}(r_{jk}) \;=\; C_j R_j(q_{j+1,k})\,Q_{j+1}(r_{jk}) < 0\,,$$

for all $k = 1, \dots, j$, and

$$(-1)^j R_{j+1}(q_{j+1,j+1}) = (-1)^j C_j R_j(q_{j+1,j+1}) > 0\,.$$

This implies that R_{j+1} has roots $r_{j+1,k},\ k = 1, \dots, j+1$, located as follows:

$$q_{j+1,k} > r_{j+1,k} > r_{jk}\,,\quad k = 1, \dots, j\,,\quad q_{j+1,j+1} > r_{j+1,j+1}\,. \tag{56}$$

Thus all roots of R_{j+1} are negative and simple.

The inequalities $p_{j+1,k} > q_{j+1,k} > r_{j+1,k}$ for all $k = 1, \dots, j+1$, follow from (54) and (56), and the inequalities $r_{j+1,k} > p_{j+1,k+1}$ for all $k = 1, \dots, j$, follow from (56) and (52). This completes the proof. □

10 Projective monodromy of the Lamé equation

Lamé equation with integer m has trivial local monodromy about the origin. Since the fundamental group of the torus is $\mathbf{Z}^2$, the projective monodromy is represented by a pair of commuting elements $PSL(2, \mathbf{C})$.

So we investigate the set pairs of commuting elements of $PSL(2)$ modulo conjugation. Every such pair (A, B) can be conjugated to one of the following forms:

$$(z \mapsto \mu_1 z,\ z \mapsto \mu_2 z), \quad (\mu_1, \mu_2) \in (\mathbf{C}^*)^2, \tag{57}$$

$$(z \mapsto z + a_1,\ z \mapsto z + a_2), \quad (a_1, a_2) \in \mathbf{C}^2, \tag{58}$$

or

$$(z \mapsto -z,\ z \mapsto 1/z). \tag{59}$$

It is proved in [9, Theorem 2.2] that the third possibility (59) cannot happen for the projective monodromy of Lamé equations with integer m. Notice that $PSL(2, \mathbf{C})$ representations (57) and (58) can be lifted to $SL(2, \mathbf{C})$. The pair $(A, B) = (\mathrm{id}, \mathrm{id})$ is also excluded.

Conjugacy classes of pairs of the form (57) are parametrized by $(\mathbf{C}^*)^2$. Two pairs of the form (58) are conjugate iff $(a_1 : a_2) = (a_1' : a_2')$, so they are parametrized by the projective line $\mathbf{CP}^1$ and one point $(0, 0)$.

Suppose that a sequence of pairs (A, B) of type (57) converges to a pair of type (58). To figure out how (a_1, a_2) in (58) are related to (μ_1, μ_2) we consider commuting pairs of linear-fractional transformations (ϕ_1, ϕ_2),

$$\phi_j(z) = \frac{(1+f_j)z + (a_j + p_j)}{q_j z + (1+g_j)}, \quad j \in \{1, 2\},$$

where f_j, g_j, p_j, q_j are small numbers, and a_j are constants not simultaneously equal to 0.

The condition that these matrices have determinant 1 gives

$$f_j + g_j \equiv a_j q_j, \tag{60}$$

where $\equiv$ means that we neglected the terms of order 2 and higher. The condition that ϕ_1 and ϕ_2 commute implies by comparing the diagonal elements of the product matrices

$$a_1 q_2 \equiv a_2 q_1. \tag{61}$$

Now it follows from (60) and (61) that

$$(f_1 + g_1) : (f_2 + g_2) \to (a_1^2 : a_2^2). \tag{62}$$

Similar equation can be obtained when the eigenvalue of one or both limit matrices is -1. In other words, if A and B are $SL(2, \mathbf{C})$ matrices representing ϕ_1 and ϕ_2 tending to parabolic ϕ_1^* and ϕ_2^*, then we have

$$\lim \frac{\operatorname{tr}^2 A - 4}{\operatorname{tr}^2 B - 4} = (a_1^2 : a_2^2), \tag{63}$$

where $(a_1 : a_2)$ is the "ratio invariant" of the pair of commuting parabolic transformations.

So we obtain that the space of projective monodromy representations for Lamé equations is the blow up of $(\mathbf{C}^*)^2$ at the point $(1, 1)$. Monodromies of unitarizable Lamé equations form the real torus

$$\{(\mu_1, \mu_2) \in (\mathbf{C}^*)^2 : |\mu_1| = |\mu_2| = 1\} \backslash (1, 1),$$

and the boundary of this real torus in the blow up is the real projective line. Since A and B are elliptic, the left hand side of (63) is positive, so the ratio $(a_1 : a_2)$ is real.

Thus we obtain

Proposition 10.1. *Abelian integrals arising as limits of developing maps of spherical metrics have real period ratios.*

11 Lin–Wang curves

Proposition 10.1 gives the following characterization of Lin–Wang curves: $J \in \pi(\mathrm{LW}_m)$ *if some Lamé equation with invariant* J *has translational monodromy which belongs to a straight line.* In particular, there is a flat singular torus corresponding to (J, λ), and this torus is of the form $\Phi^*(T)$ where T is a BFT with integer angles.

Proof of Theorem 1.3.

The set LW_m is the image of the set of triangles with angles integer multiples of π under the map Φ^*_m. Triangles with angles integer multiples of π form straight intervals in the local coordinates $\phi_{i,j,k}$ introduced in Section 4, and the map Φ^*_m is biholomorphic.

We conclude that the set LW_m consists of analytic (non-singular) curves. There are three such curves corresponding to each integer point in $\mathbf{A}_m$. So all together we have $m(m+1)/2$ Lin–Wang curves. □

Proposition 10.1 shows how to find equations of Lin–Wang curves. They are curves in $\mathbf{L}_m$ the Lamé spectral curve where the ratio of periods of the integral (23) is real. According to [14], to each triple of integers satisfying the triangle inequalities corresponds a component of the space $\mathrm{Sph}_{1,1}(2m+1)$. This component is parametrized by an open triangle, and the sides of this triangle correspond to three interior edges of $\mathbf{T}_m$ which are mapped by ϕ in (34) to integer points of $\mathbf{A}_m$ by the map ϕ in (34). These three edges parametrize Lin–Wang curves by the map $\pi_m \circ \Phi^*_m$.

Thus each integer point in $\mathbf{A}_m$ corresponds to a component of the moduli space of $\mathrm{Sph}_{1,1}(m)$ of spherical tori. The boundary of this component consists of one or three Lin–Wang curves: when the integer point is the center of $\mathbf{A}_m$, which happens when $m \equiv 1 \pmod 3$, there is one curve, otherwise there are three of them. If there is one curve, it belongs to $\mathbf{L}^{II}_m$, as it happens for $m = 1$ and $m = 4$.

For integer points other than the center of $\mathbf{A}_m$ we have three curves which can be all on component $\mathbf{L}^{II}_m$, or one of them can be on $\mathbf{L}^{I}_m$ and two on $\mathbf{L}^{II}_m$. Figs. 6, 7 and similar figures for other m permits to determine this for every integer point on $\mathbf{A}_m$.

We give the explicit formulas for Lin–Wang curves for $1 \le m \le 3$. We recall that the developing map is given by (19). Since working with elliptic functions is easier than with Abelian integrals (this was the primary reason

for introducing elliptic functions), we pass to the universal covering.

In what follows, g is the integrand in (19). It is an even elliptic function with a single zero of multiplicity $2m$ at the origin, and double poles with vanishing residues. The general form of such function is

$$g(z) = c_0 + \sum_{j=1}^{m} c_j \wp(z - a_j).$$

By Abel's theorem, $2(a_1 + \ldots + a_m) \equiv 0$, and we want to choose c_j so that g and its first $2m-1$ derivatives vanish at the origin. So

$$c_0 = -\sum_{j=1}^{m} c_j \wp(a_j),$$

and for the rest of c_j we have a system of equations

$$\sum_{j=1}^{m} c_j \wp^{(k)}(-a_j) = 0, \quad 1 \le k \le 2m-1,$$

which has a non-trivial solution if the matrix of this system has rank at most $m-1$.

Once g is found, we are interested in the ratio of periods of the integral (19). Lin–Wang curves make the locus of points where this ratio is real. Below we give the results of computation for $1 \le m \le 3$. We use the standard notation of the theory of elliptic functions [1]: $\wp(\omega_j) = e_j$, $1 \le j \le 3$, so ω_j are half-periods, ζ is the Weierstrass zeta function, $\zeta' = -\wp$, satisfying

$$\zeta(z + \omega_j) = \zeta(z) + \eta_j.$$

Case $m = 1$. $g(z) = \wp(z - \omega_j) - e_j$, $j \in \{1, 2, 3\}$. In this case, $\mathbf{L}_1 = \mathbf{L}_1^{II}$. The equation of Lin–Wang curves is

$$\operatorname{Im} \frac{\eta_1 + \omega_1 e_j}{\eta_2 + \omega_2 e_j} = 0, \quad j \in \{1, 2, 3\}.$$

This defines three curves in the fundamental region of the modular group in the τ-half-plane, Fig. 12, which correspond to one curve in the J-plane (Fig. 13).

Case $m = 2$. For $\mathbf{L}_2^I$, we obtain

$$g(z) = \wp(z+a) + \wp(z-a) - 2\wp(a), \quad \text{where} \quad \wp(a) = \sqrt{g_2/12}.$$

The equation of the Lin–Wang curve is

$$\operatorname{Im} \frac{\eta_1 + \omega_1\sqrt{g_2/12}}{\eta_2 + \omega_2\sqrt{g_2/12}} = 0.$$

For $\mathbf{L}_2^{II}$, we have

$$g(z) = \wp''(\omega_j)\left(\wp(z+\omega_k) - e_k\right) - \wp''(\omega_k)\left(\wp(z+\omega_j) - e_j\right),$$

and the equation of Lin–Wang curve is

$$\operatorname{Im} \frac{\omega_1(e_j\wp''(\omega_k) - e_k\wp''(\omega_j)) + \eta_1(\wp''(\omega_k) - \wp''(\omega_j))}{\omega_2(e_j\wp''(\omega_k) - e_k\wp''(\omega_j)) + \eta_2(\wp''(\omega_k) - \wp''(\omega_j))} = 0.$$

These curves in the τ-half-plane are shown in Fig. 14 and their images in the J-plane are in Fig. 15. These are the three curves bounding a single triangle which is the moduli space $\mathrm{Sph}_{1,1}(5)$. One of these curves, (which has a loop in Fig. 12) belongs to $\mathbf{L}_2^I$, other two belong to $\mathbf{L}_2^{II}$. Shading in Fig. 15 is the *hypothetical* projection of a component of $\mathrm{Sph}_{1,1}(5)$ by the forgetful map. We do not know whether the restriction of the forgetful map on $\mathrm{Sph}_{1,1}(2m+1)$ is open. So we don't know that the boundary of this projection is contained in Lin–Wang curves.

Case $m = 3$. For $\mathbf{L}_3^I$ we obtain:

$$g(z) = c_0 + c_1\wp(z+\omega_1) + c_2\wp(z+\omega_2) + c_3\wp(z+\omega_3),$$

where

$$c_0 = -\sum_{j=1}^{3} c_j e_j,$$

$$c_k = (6e_{k+2}^2 - g_2/2)(6e_{k+1}^2 - g_2/2)(e_{k+2} - e_{k+1}), \quad k \in \{1,2,3\},$$

where the subscripts are understood as residues mod 3, but we use 3 instead of 0 to prevent the confusion with previous formula. Setting $B = c_1 + c_2 + c_3$, the equation of the Lin-Wang curve is

$$\operatorname{Im} \frac{\omega_1 c_0 - \eta_1 B}{\omega_2 c_0 - \eta_2 B} = 0.$$

This curve in the τ-plane is shown in Fig. 16.

For component $\mathbf{L}_3^{II}$ we introduce the notation for $k \in \{1,2,3\}$:

$$P_k^{\pm} = -e_k/5 \pm \sqrt{3(5g_2/4 - 3e_k^2)},$$

$$c_{1,k}^{\pm} = -2\frac{6(P_k^{\pm})^2 - g_2/2}{6e_k^2 - g_2/2},$$

$$c_{0,k}^{\pm} = -c_{1,k}^{\pm} e_k - 2P_k^{\pm}.$$

Then

$$g(z) = c_{0,k}^{\pm} + c_{1,k}^{\pm}\wp(z+\omega_k) + \wp(z+a_k^{\pm}) + \wp(z-a_k^{\pm}),$$

where $\pm a_k^{\pm}$ are solutions of the equation $\wp(z) = P_k^{\pm}$. Then we have six Lin–Wang curves

$$\operatorname{Im}\frac{c_{0,k}^{\pm}\omega_1 - (c_{1,k}^{\pm}+2)\eta_1}{c_{0,k}^{\pm}\omega_2 - (c_{1,k}^{\pm}+2)\eta_2} = 0.$$

These curves in the τ-half-plane are shown in Fig. 17, and their image in the J-plane in Fig. 18, where the curve from $\mathbf{L}_3^I$ is also included (it is the one which looks like a vertical line in the middle). Fig. 18 shows in the right-hand side the detail which looks like a tripod in the left-hand side. Figure 17 contains 16 curves which give 5 images in Fig. 18. Three of these 5 curves in Fig. 18 constitute the full boundary of one triangle of the moduli space for spherical tori, and the remaining three curves in Fig. 18, including that one curve which comes from Fig. 16 constitute the boundary of the second triangle in the moduli space for spherical tori.

Appendix. List of formulas

Polynomials F_m^I:

2	$\lambda^2 - 3g_2$
3	λ
4	$\lambda^3 - 52g_2\lambda + 560g_3$
5	$\lambda^2 - 27g_2$
6	$\lambda^4 - 294g_2\lambda^2 + 7776g_3\lambda + 3465g_2^2$
7	$\lambda^3 - 196g_2\lambda + 2288g_3$
8	$\lambda^5 - 1044g_2\lambda^3 + 48816g_3\lambda^2 + 112320g_2^2\lambda - 4665600g_2g_3$
9	$\lambda^4 - 774g_2\lambda^2 + 21600g_3\lambda + 41769g_2^2$.

Polynomials F_m^{II}:

1	$4\lambda^3 - g_2\lambda - g_3$
2	$4\lambda^2 - 9g_2\lambda + 27g_3$
3	$16\lambda^6 - 504g_2\lambda^4 + 2376g_3\lambda^3 + 4185g_2^2\lambda^2 - 36450g_2g_3\lambda - 3375g_2^3 + 91125g_3^2$
4	$16\lambda^6 - 1016g_2\lambda^4 + 8200g_3\lambda^3 + 10297g_2^2\lambda^2 - 41650g_2g_3\lambda$ $-27783g_2^3 - 42875g_3^2$.

Polynomials H_m^0:

2	$B^2 + 4(a+1)B + 12a$
3	$B + 4(a+1)$
4	$B^3 + 20(a+1)B^2 + (64a^2 + 336a + 64)B + 640(a^2 + a)$
5	$B^2 + 20(a+1)B + 64(a^2+1)$
6	$B^4 + 56(a+1)B^3 + (784a^2 + 2744a + 784)B^2$ $+(2304a^3 + 29472a^2 + 29472a + 2304)B$ $+48384a^3 + 152208a^2 + 48384a$

Polynomials H_m^1:

1	$B + a + 1$
2	$B + 4a + 1$
3	$B^2 + 10(a+1)B + 9a^2 + 78a + 9$
4	$B^2 + (20a+10)B + 64a^2 + 136a + 9$
5	$B^3 + 35(a+1)B^2 + (259a^2 + 1046a + 259)B$ $+225a^3 + 5235(a^2+a) + 225$
6	$B^3 + (56a+35)B^2 + (784a^2 + 1568a + 259)B$ $+2304a^3 + 13008a^2 + 7464a + 225$

Degrees of forgetful maps:

$$d_m^I := \begin{cases} m/2+1, & m \equiv 0 \pmod 2 \\ (m-1)/2, & m \equiv 1 \pmod 2, \end{cases} \tag{64}$$

$$d_m^{II} := 3\lceil m/2 \rceil. \tag{65}$$

Euler characteristics:

$$\chi(\mathbf{L}_m^I) = \begin{cases} -\dfrac{(m+2)^2}{24} + \dfrac{4\epsilon_0 + 3\epsilon_1}{6}, & m \equiv 0 \pmod 2, \\ -\dfrac{(m-1)^2}{24} + \dfrac{4\epsilon_0 + 3\epsilon_1}{6}, & m \equiv 1 \pmod 2. \end{cases}$$

$$\chi(\mathbf{L}_m^{II}) = \begin{cases} -\dfrac{m^2}{8} + \dfrac{1-\epsilon_1}{2}, & m \equiv 0 \pmod 2, \\ -\dfrac{(m+1)^2}{8} + \dfrac{1-\epsilon_1}{2}, & m \equiv 1 \pmod 2. \end{cases},$$

where

$$\epsilon_0 = \begin{cases} 0, & \text{if } m \equiv 1 \pmod 3, \\ 1 & \text{otherwise,} \end{cases}$$

$$\epsilon_1 = \begin{cases} 0, & \text{if } m \in \{1, 2\} \pmod 4, \\ 1 & \text{otherwise.} \end{cases}$$

Numbers of punctures: $h_m^I = d_m^I,\ h_m^{II} = 2d_m^{II}/3$.
Genera in terms of d_m^K:

$$g(\mathbf{L}_m^I) = 1 + \frac{(d_m^I)^2}{12} - \frac{d_m^I}{2} - \frac{4\epsilon_0 + 3\epsilon_1}{12}, \tag{66}$$

$$g(\mathbf{L}_m^{II}) = 1 + \frac{(d_m^{II})^2}{36} - \frac{d_m^{II}}{3} - \frac{1-\epsilon_1}{4}. \tag{67}$$

Genera in terms of m:

$$g(\mathbf{L}_m^I) = \frac{m^2 - 8m + 28}{48} - \frac{4\epsilon_0 + 3\epsilon_1}{12}, \quad m \equiv 0 \pmod 2, \tag{68}$$

$$g(\mathbf{L}_m^I) = \frac{m^2 - 14m + 61}{48} - \frac{4\epsilon_0 + 3\epsilon_1}{12}, \quad m \equiv 1 \pmod 2, \tag{69}$$

$$g(\mathbf{L}_m^{II}) = \frac{m^2 - 8m + 16}{16} - \frac{1-\epsilon_1}{4}, \quad m \equiv 0 \pmod 2, \tag{70}$$

$$g(\mathbf{L}_m^{II}) = \frac{m^2 - 6m + 9}{16} - \frac{1-\epsilon_1}{4}, \quad m \equiv 1 \pmod 2. \tag{71}$$

Degrees of Cohn's polynomials

$$\deg C_m^I = \left\lfloor \frac{(d_m^I)^2 - d_m^I + 4)}{6} \right\rfloor,$$

$$\deg C_m^{II} = \frac{d_m^{II}(d_m^{II} - 1)}{2}.$$

References

[1] N. I. Akhiezer, Elements of the theory of elliptic functions, AMS, Providence, RI, 1990.

[2] M. Bainbridge, D. Chen, Q. Gendron, S. Grushevsky and M. Möller, Strata of k-differentials. Alg. Geom. 6 (2019) 196–233.

[3] M. Bainbridge, D. Chen, Q. Gendron, S. Grushevsky and M. Möller, Compactification of strata of Abelian differentials, Duke Math. J., 167, 12 (2018) 2348–2416.

[4] W. Bergweiler and A. Eremenko, Green functions and antiholomorphic dynamics on tori, Proc. AMS 144 N 7 (2016) 2911–2922.

[5] C. Boissy, Connected components of the strata of the moduli space of meromorphic differentials, Comment. Math. Helv. 90 (2015) 255–286.

[6] MathOverflow, Examples of plane algebraic curves, https://mathoverflow.net/questions/352957.

[7] A. Bonifant and J. Milnor, Group actions, divisors, and plane curves, Bull. AMS 57, 2 (2020) 171–267.

[8] E. Brieskorn and H. Knörrer, Plane algebraic curves, Birkhäuser/Springer, Basel, 1986.

[9] C.-L. Chai, C.-S. Lin, C.-L. Wang, Mean field equations, hyperelliptic curves and modular forms: I, Camb. J. Math. 3 (2015), no. 1-2, 127-274.

[10] C.-L. Chai, C.-S. Lin and C.-L. Wang, Mean field equations, hyperelliptic curves and modular forms: II, J. Éc. polytech. Math. 4 (2017), 557-593.

[11] Z. Chen and C.-S. Lin, Critical points of the classical Eisenstein series of weight two, J. Differential Geom. 113 (2019), no. 2, 189-226.

[12] A. Eremenko, Metrics of positive curvature with conic singularities on the sphere, Proc. Amer. Math. Soc. 132 N 11 (2004) 3349–3355.

[13] A. Eremenko and A. Gabrielov, Rational functions with real critical points and the B. and M. Shapiro conjecture in real enumerative geometry, Ann of Math. 155 (2002), 105–129.

[14] A. Eremenko, G. Mondello and D. Panov, Moduli of spherical tori with one conical point, in preparation.

[15] R. Gantmakher and M. Krein, Oscillation matrices and kernels and small vibrations of mechanical systems, AMS Chelsea, Providence, RI, 2002.

[16] T. Hosgood, An introduction to varieties in weighted projective space, arXiv:1604.02441.

[17] F. Klein, Vorlesungen über die hypergeometrische Funktion, Springer-Verlag, Göttingen, 1981 (reprint of the 1933 edition).

[18] M. Kontsevich and A. Zorich, Connected components of the moduli spaces of Abelian differentials with prescribed singularities, Invent. math. 153 (2003) 631–678.

[19] G. Lamé, Mémoire sur les axes des surfaces isothermes du second degré considéré comme des fonctions de la température, J. de Math. pures et appl. IV (1839) 100–125.

[20] G. Lamé, Mémoire sur l'equilibre des températures dans un ellipsoïde à troi axes inégaux, J. de Math. pures et appl. IV (1839) 126–163.

[21] C.-S. Lin, Green function, mean field equation and Painlevé VI equation, in the book: Current developments in mathematics, 2015, Intl. Press, 2017.

[22] C.-S. Lin and C.-L. Wang, Elliptic functions, Green functions and the mean field equations on tori, Ann. of Math. (2) 172 (2010), no. 2, 911–954.

[23] R. Maier, Lamé polynomials, hyperelliptic reductions and Lamé band structure, Phil. Trans. R. Soc. A 366 (2008) 1115–1153.

[24] F. Loray and D. Marin, Projective structures and projective bundles over compact Riemann surfaces, Astérisque No. 323 (2009), 223-252.

[25] G. Mondello and D. Panov, Spherical metrics with conical singularities on 2-sphere: angle constraints, IMRN 16 (2016) 4937–4995.

[26] G. Mondello and D. Panov, Spherical surfaces with conical points: systole inequality and moduli spaces with many connected components, GAFA 29 4 (2019) 1110–1193.

[27] W. Thurston, On the combinatorics of iterated rational maps, preprint, Princeton U. 1985.

[28] B. Shapiro and M. Tater, On spectral asymptotics of quasi-exactly solvable quartic and Yablonskii–Vorob'ev polynomials, arXiv:1412.3026.

[29] A. Turbiner, Lamé equation, sl(2) algebra and isospectral deformations, J. Phys. A 22 (1989) L1–L3.

[30] E. T. Whittaker and G. N. Watson, A course of modern analysis, Cambridge UP, 1927.

[31] A. Zorich, Flat surfaces, in: Frontiers in Number Theory, Physics, and Geometry. I, Springer-Verlag, New York, 2006, pp. 437-583.

A. E. and A. G.: Purdue University, West Lafayette, IN 47907 USA
G. M.: "Sapienza" Università di Roma, Rome, Italy
D. P.: Kings College, London UK

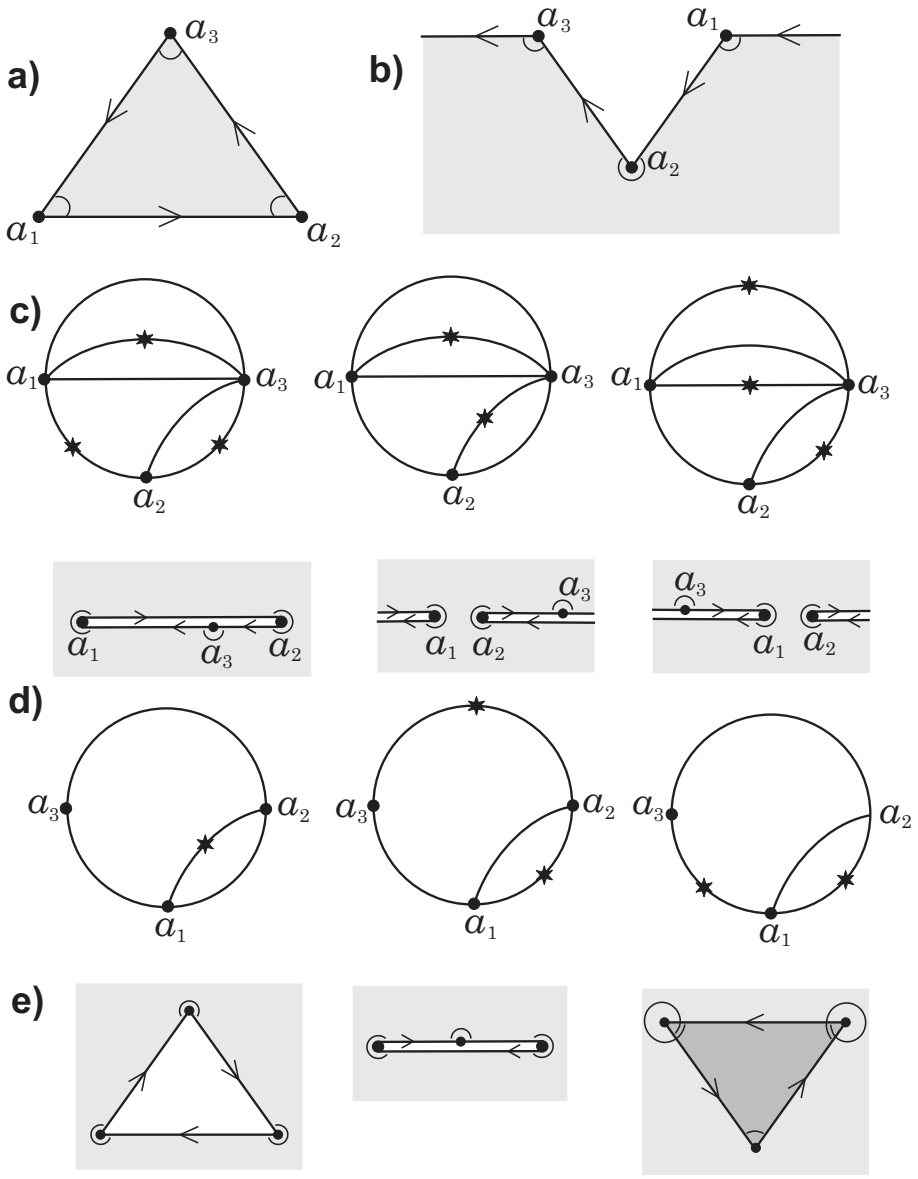

Figure 1: a),b) - primitive triangles; c) - examples of nets with the angles $(3\pi, 2\pi, 4\pi)$; d) - triangles with the angles $(2\pi, \pi, 2\pi)$ and their nets; e) - deformation of triangle with the angle sum $5\pi/3$.

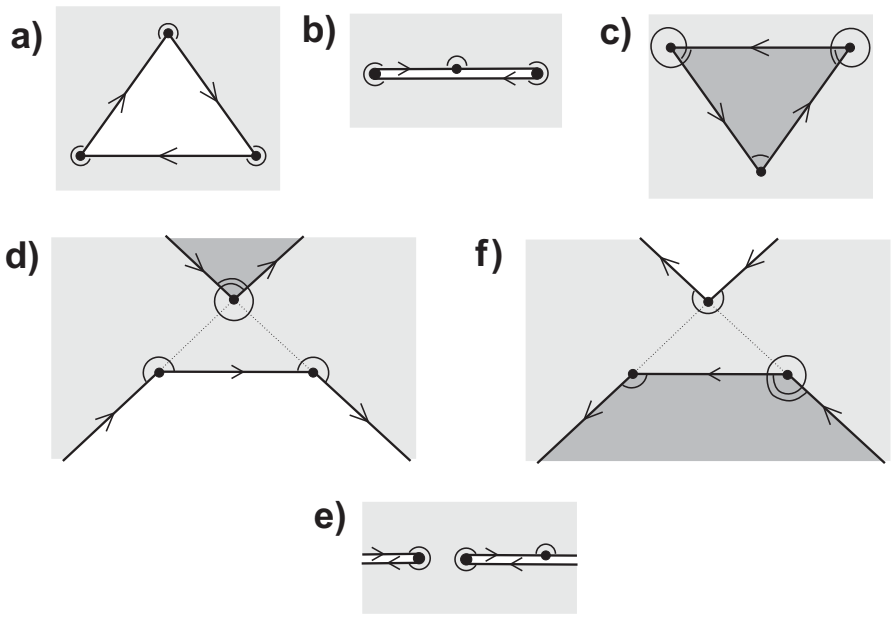

Figure 2: All types of BFT for $m = 2$.

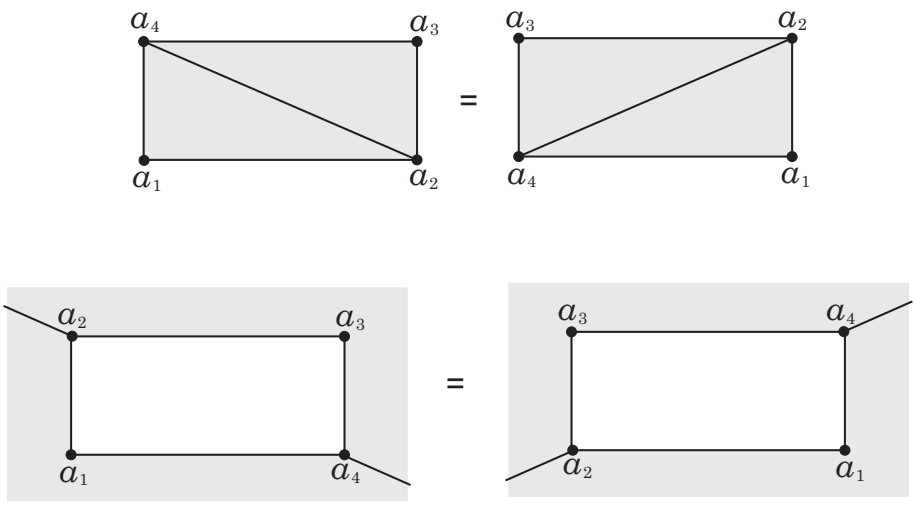

Figure 3: To the proof of Proposition 3.4.

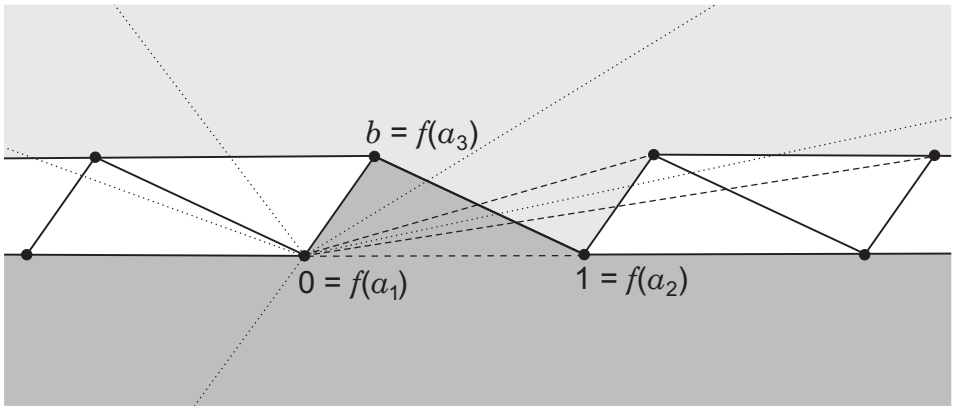

Figure 4: To the proof of Lemma 4.1 for a triangle of type A''.

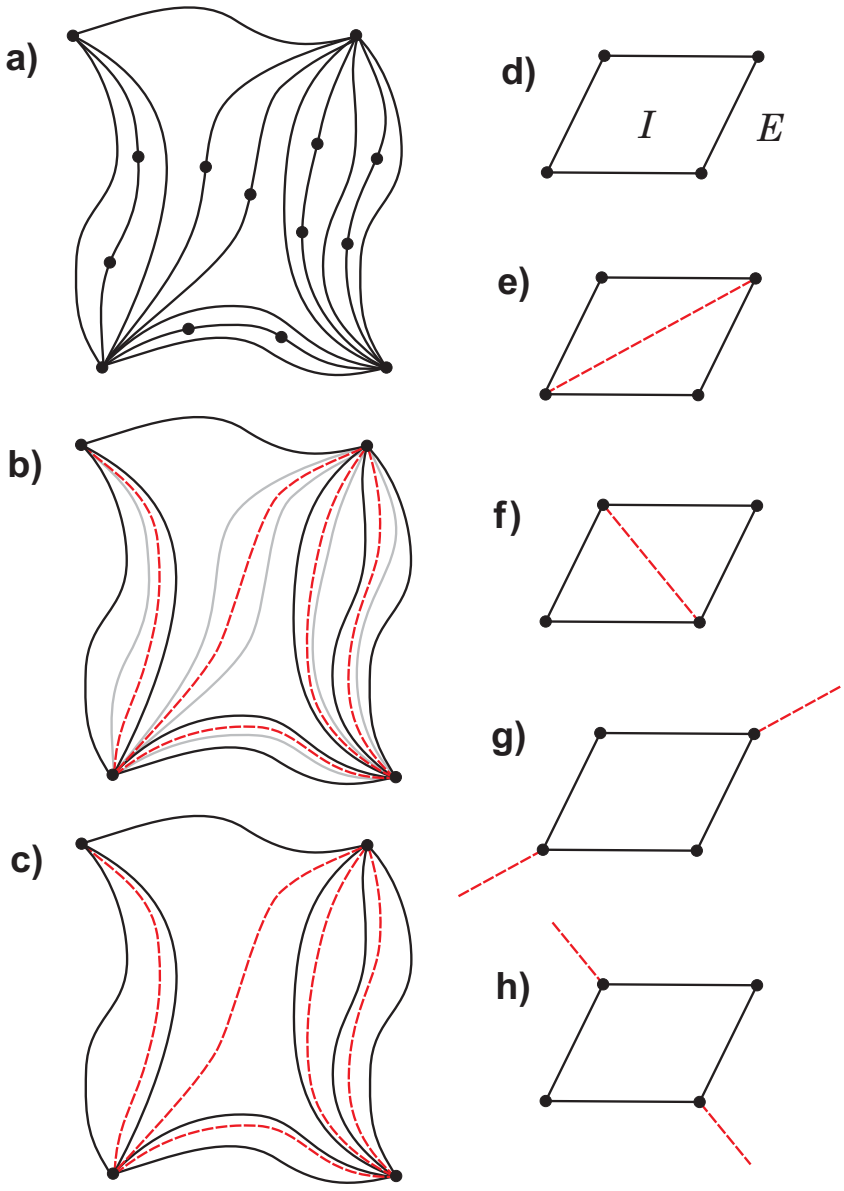

Figure 5: To the proof of Lemma 5.2.

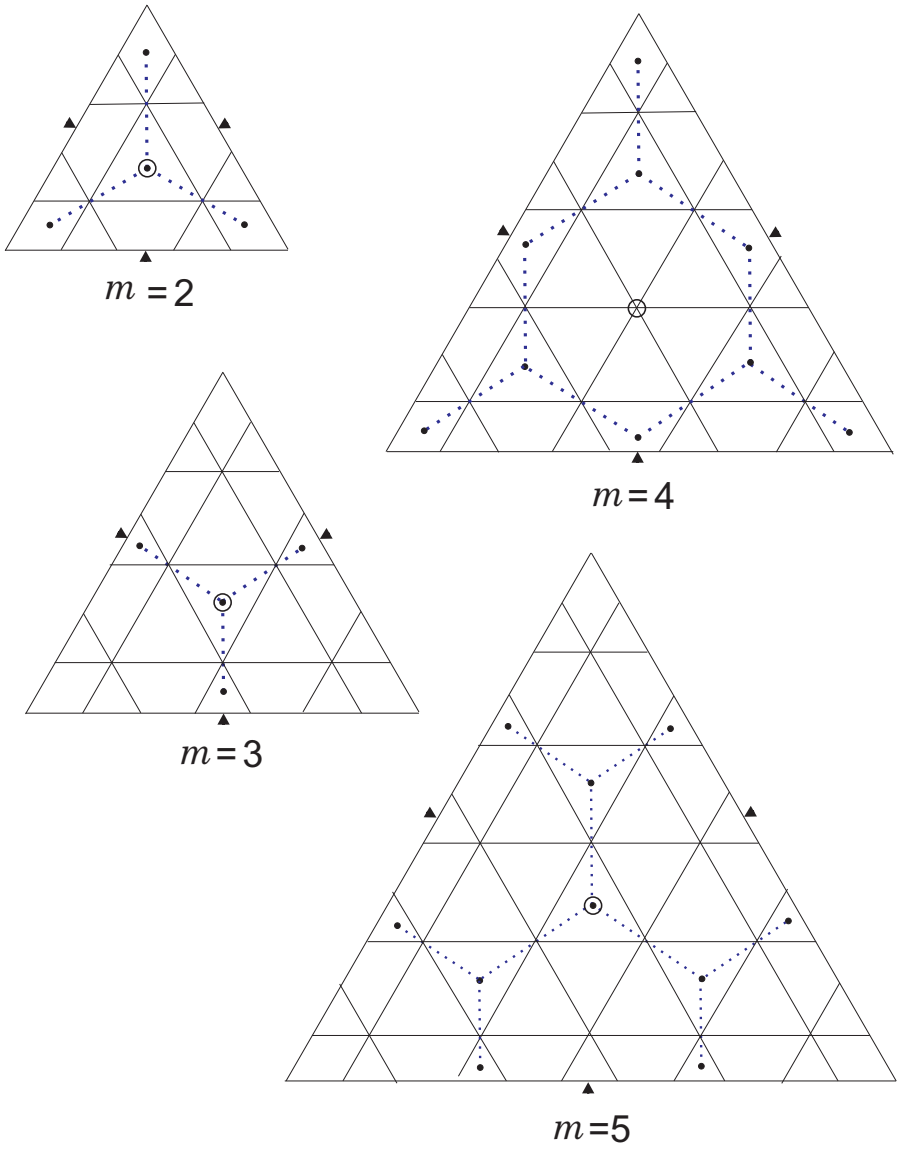

Figure 6: Spaces of angles $\mathbf{A}_m$ for $m \leq 5$. The nerve of component $\mathbf{L}_m^I$ is blue/dotted.

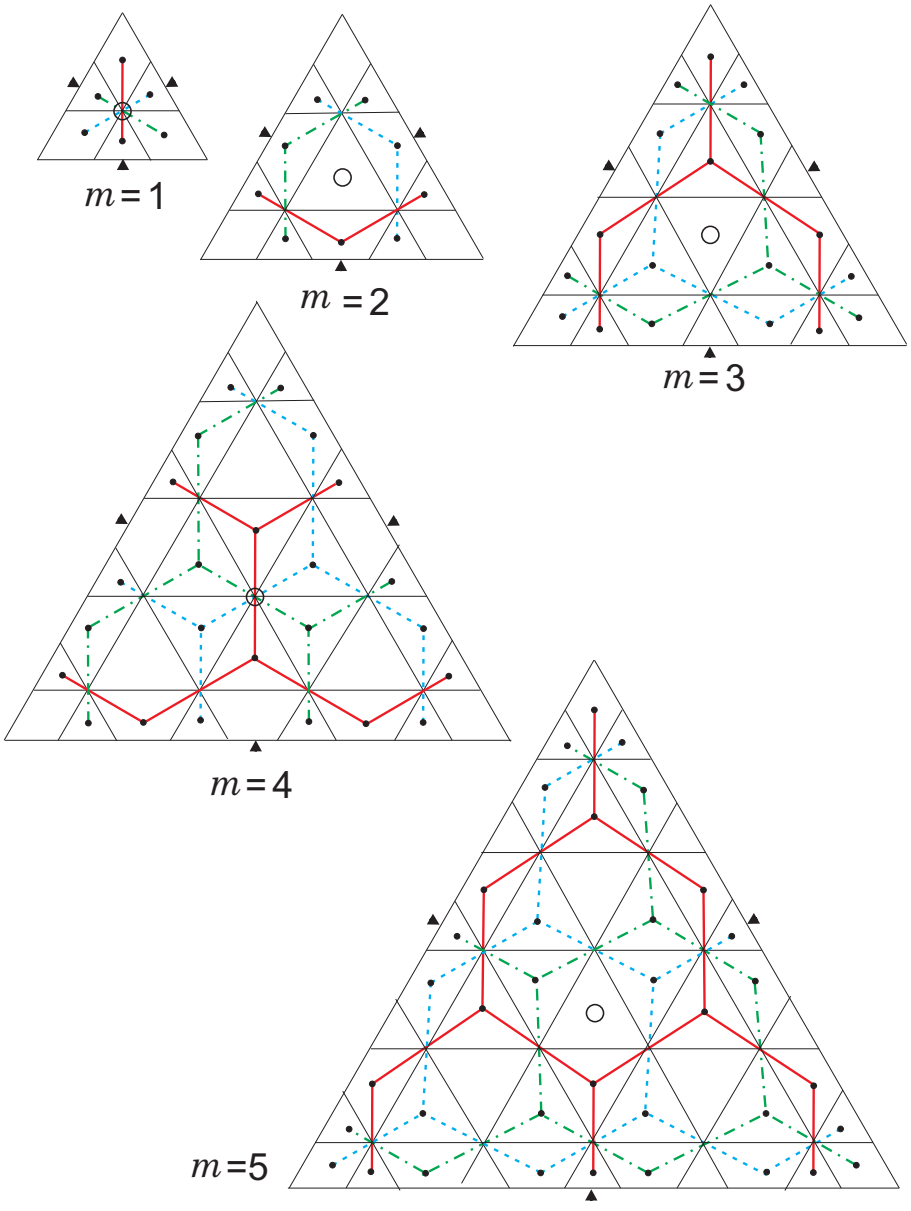

Figure 7: Spaces of angles $\mathbf{A}_m$ for $m \leq 5$. The nerves of components IIA, IIB, IIC are shown.

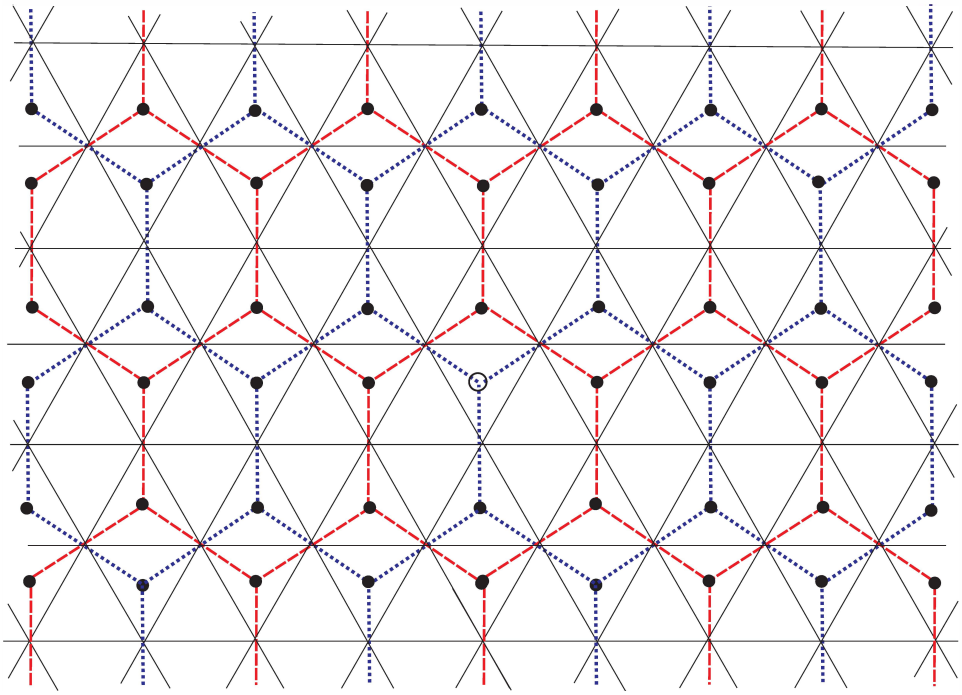

Figure 8: Two components in the space of flat singular triangles.

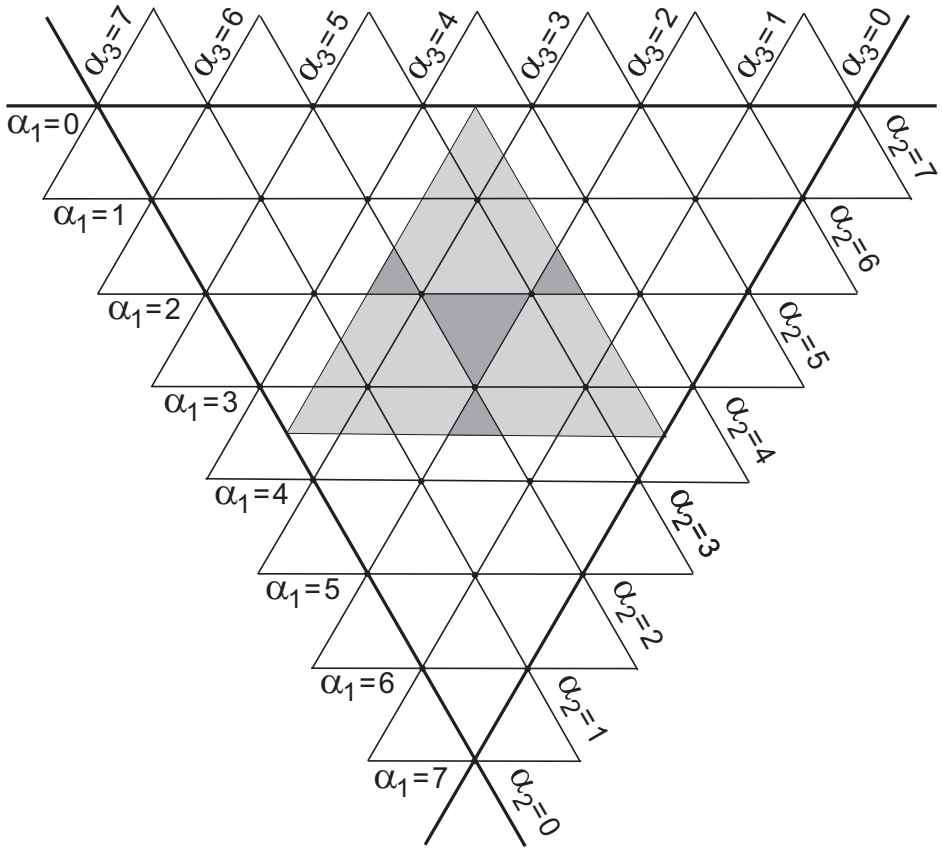

Figure 9: Triangle Δ_2 (shaded) in the intersection of the plane $\alpha_1+\alpha_2+\alpha_3 = 7$ with the first octant. Faces of type I have darker shading.

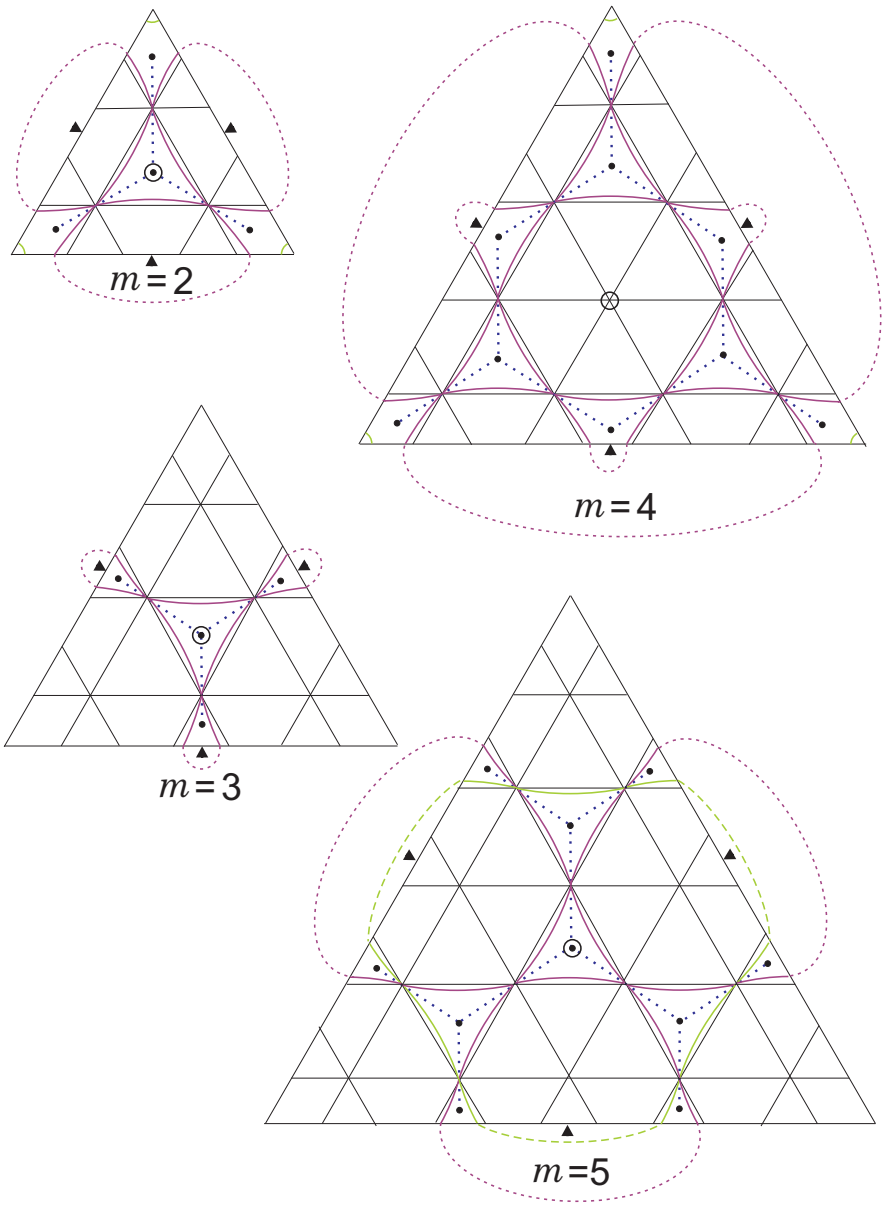

Figure 10: Counting punctures for $\mathbf{L}_m^I$.

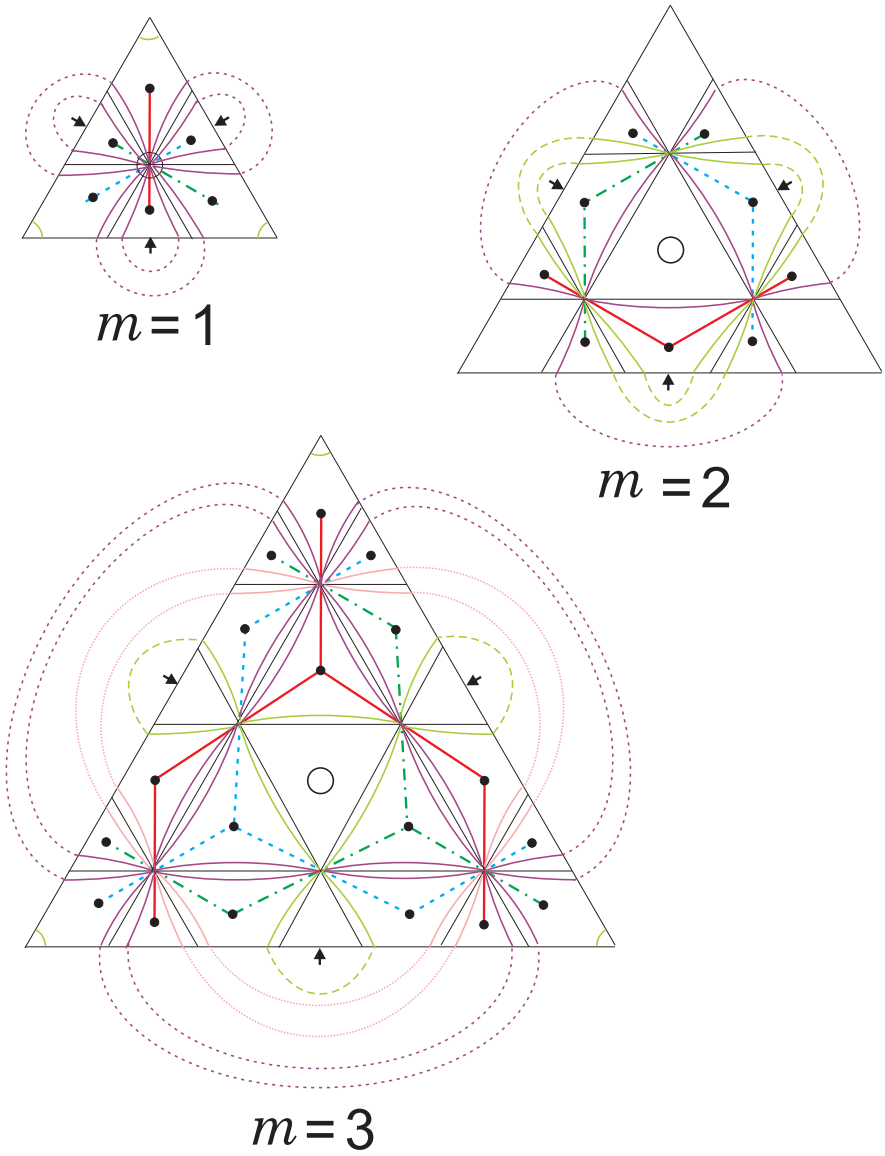

Figure 11: Counting punctures for $\mathbf{L}_m^{II}$. Dotted lines represent gluings.

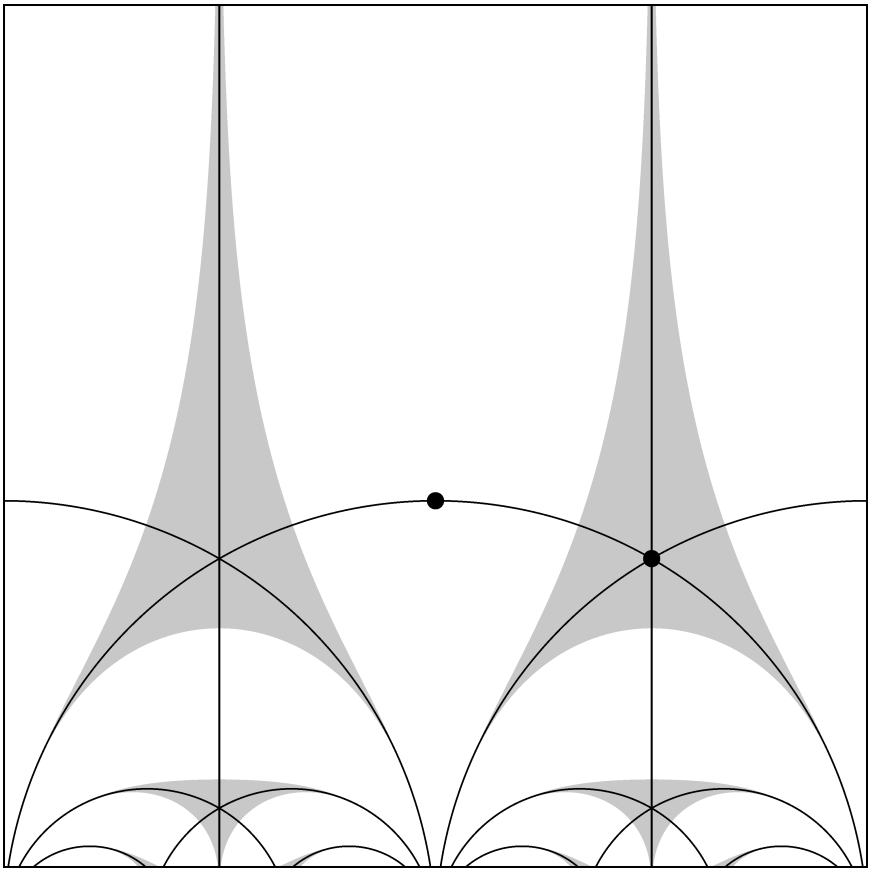

Figure 12: Lin–Wang curves for $m = 1$, τ-half-plane. Shaded area corresponds to $\mathrm{Sph}1, 1(3)$.

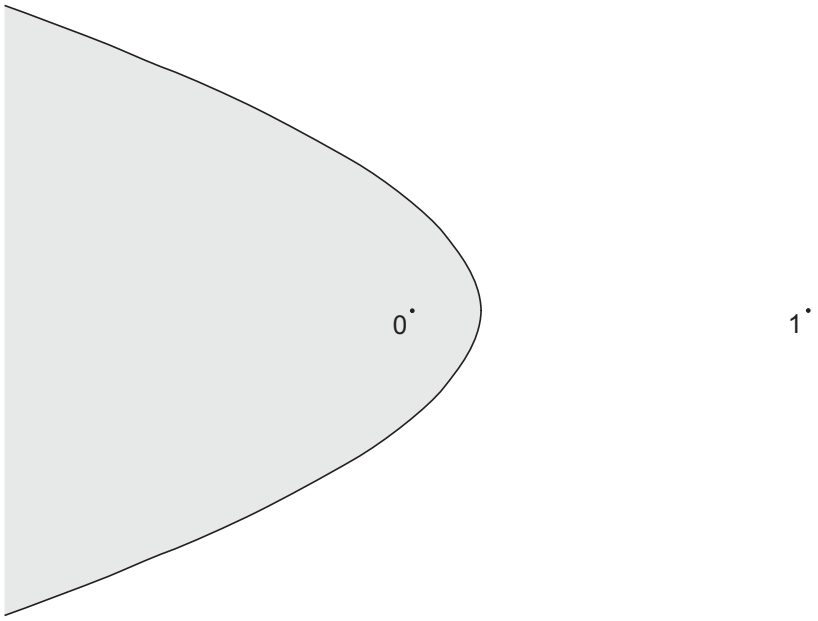

Figure 13: Lin–Wang curve $m = 1$, J-plane. Projection of $\mathrm{Sph}_{1,1}(3)$ is shaded.

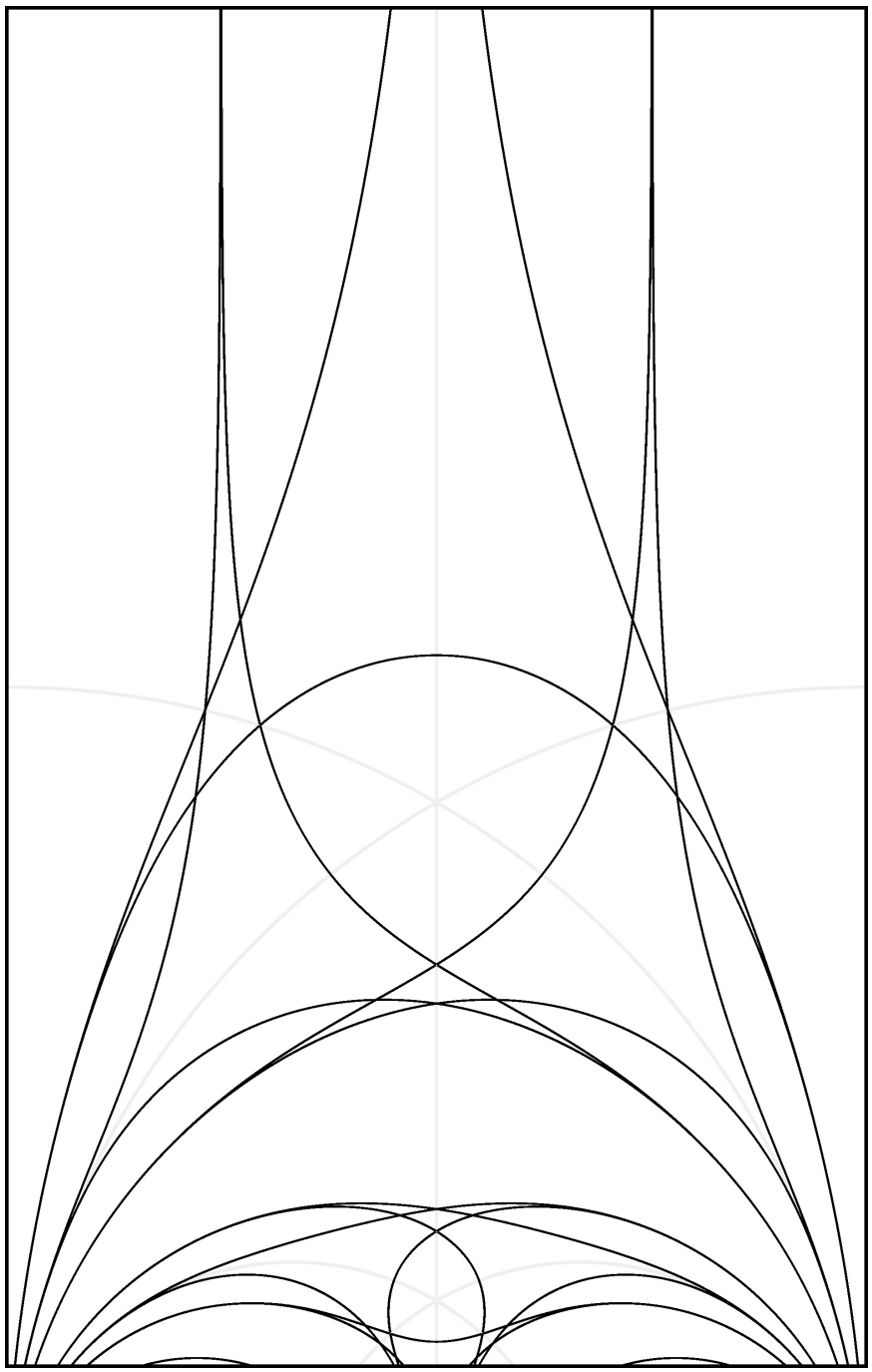

Figure 14: Lin–Wang curves for $m = 2$, τ-half-plane.

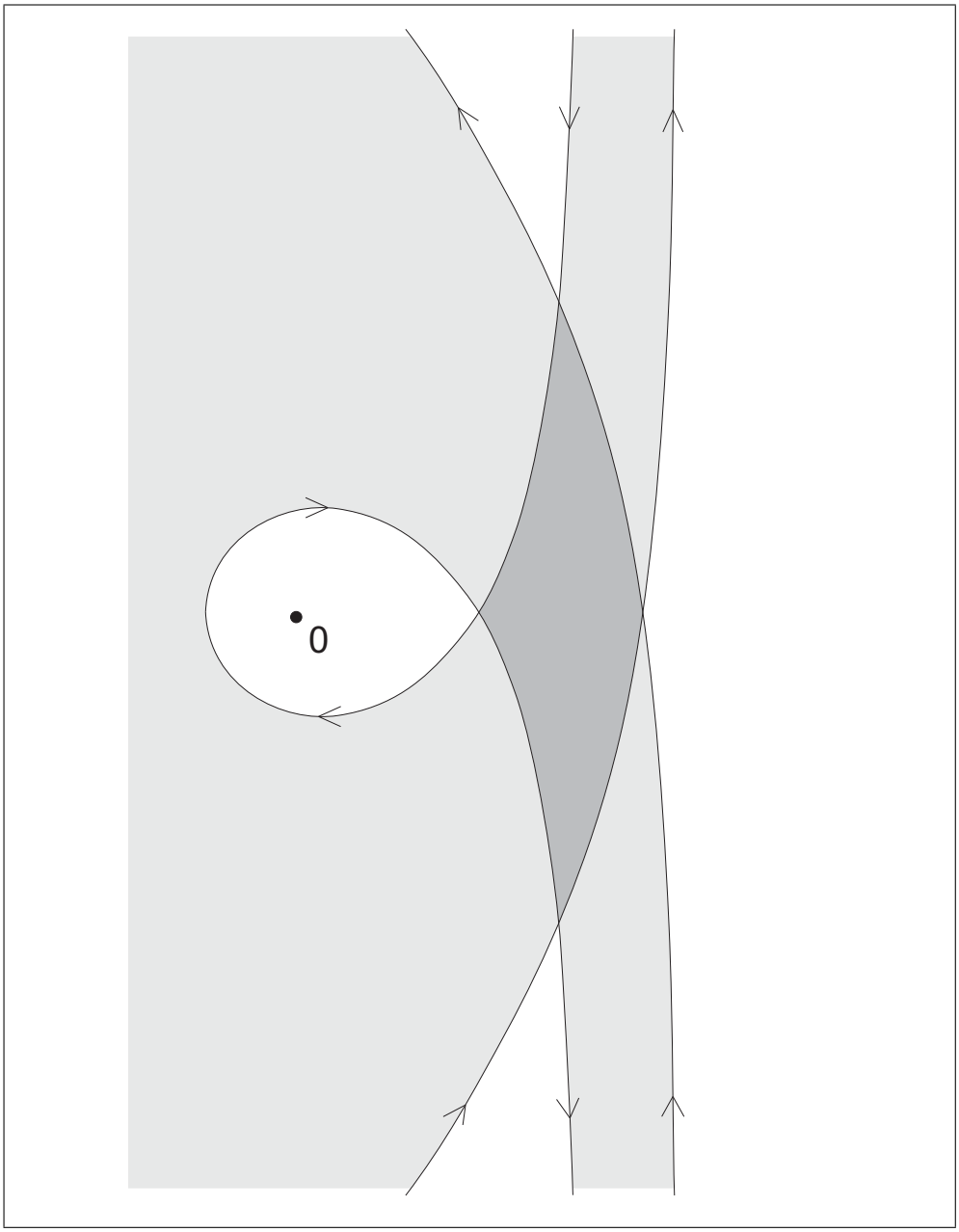

Figure 15: $m = 2$, J-plane. The curve with a loop is in $\mathbf{L}_2^I$, the other two curves in $\mathbf{L}_2^{II}$. Shaded area is the *hypothetical* projection of $\mathrm{Sph}_{1,1}(5)$; it is not known whether the restriction of the forgetful map on $\mathrm{Sph}_{1,1}(5)$ is open.

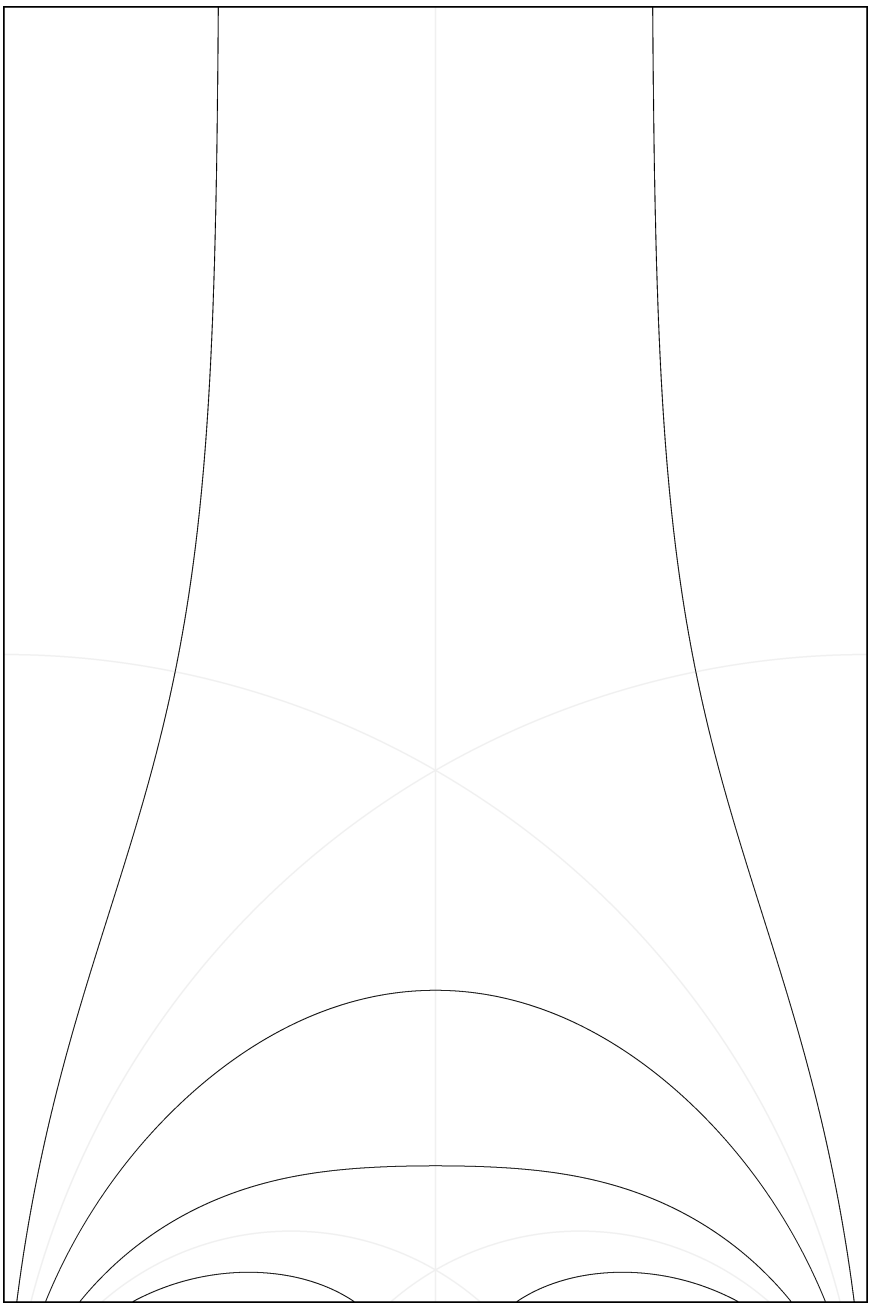

Figure 16: $m = 3$, τ-half-plane, Lin–Wang curves from $\mathbf{L}_3^I$.

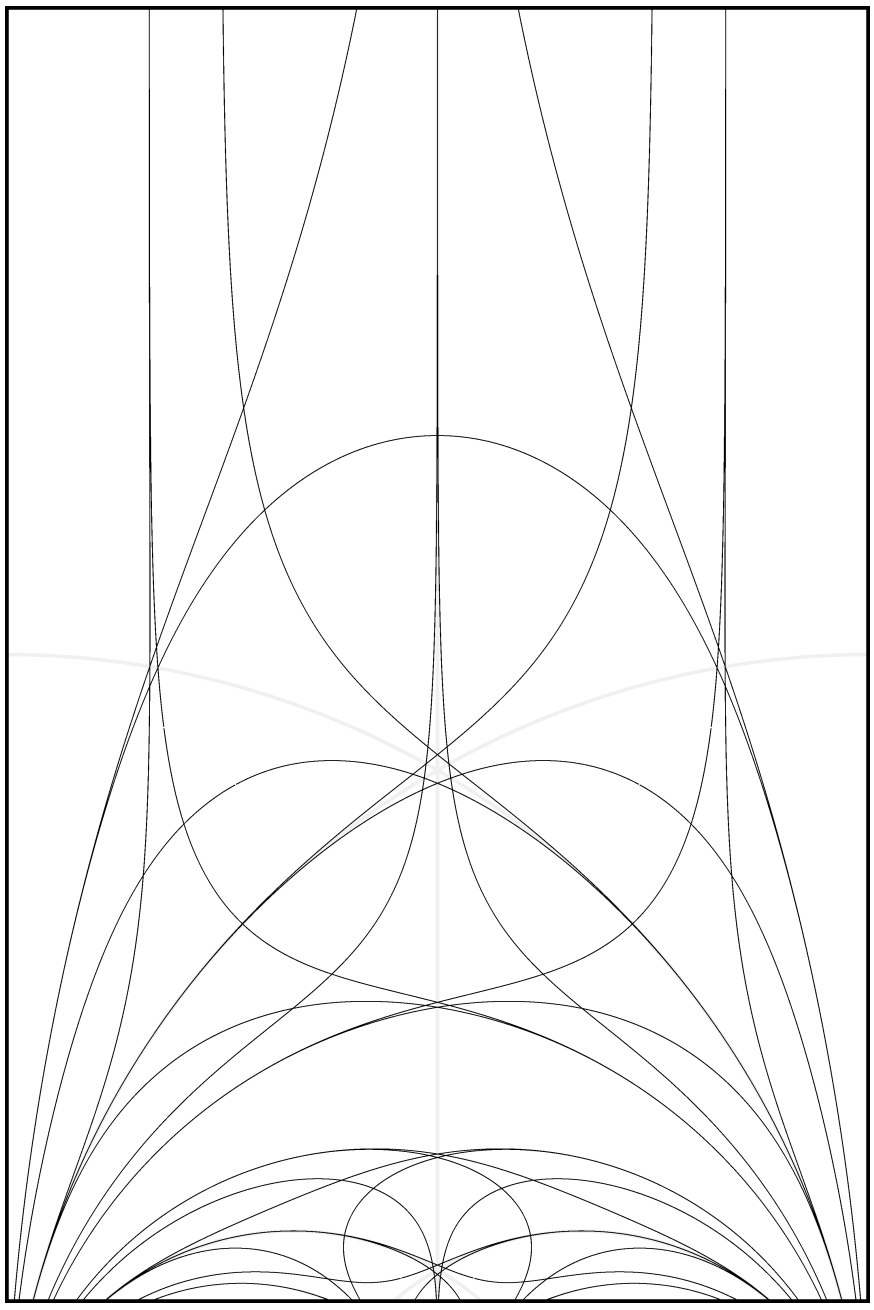

Figure 17: $m = 3$, τ-half-plane, Lin–Wang curves from $\mathbf{L}_3^{II}$.

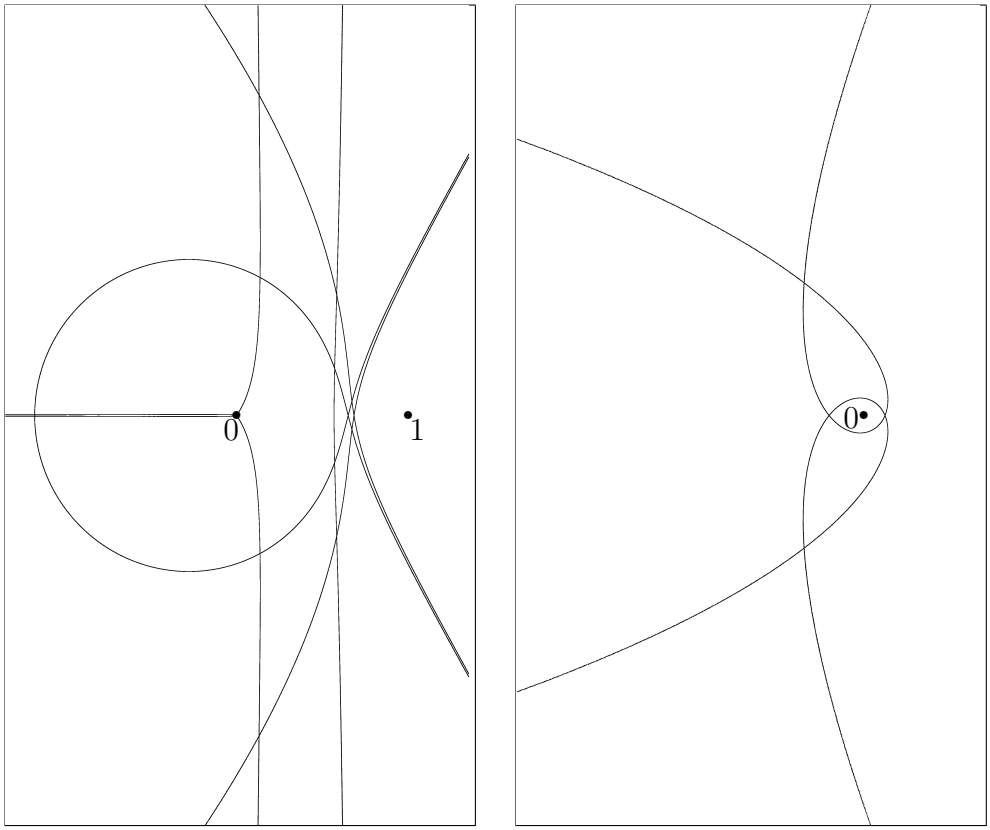

Figure 18: $m = 3$, J-plane, Lin–Wang curves from both components. Magnification of detail on the right, this detail is on component $\mathbf{L}_3^{II}$.